

Radiation Monitoring Devices, Inc.
44 Hunt Street
Watertown, MA 02172
(617) 926-1167

SOFT X-RAY WINDOW ENCAPSULANT FOR HgI₂ DETECTORS - PHASE II

June 30, 1987

PROJECT SUMMARY - CONTRACT NO. NAS7-931

For many years HgI₂ has appeared to be an ideal material for use in uncooled x-ray and gamma ray detectors. This is because it is a wide band gap semiconductor which permits room temperature operation. It has a high average atomic number and high density which gives it very good stopping power for x-rays and gamma rays. Most importantly, crystals can be grown with excellent electronic properties including moderately good electron and hole transport and high sensitivity. These are exactly the properties needed for making sensitive, low noise, solid state x-ray sensors.

HgI₂ devices, however, have been plagued by instability problems which have prevented their use. Detector performance degrades rapidly after fabrication, often within a few days or weeks. HgI₂ technology has matured to the point where excellent crystals and devices can be produced by a number of techniques. In addition, recent advances in low noise electronic preamplifiers has made the construction of sensitive, high resolution HgI₂ spectrometers possible. Thus, device instability was the major remaining obstacle which prevented the implementation of useful HgI₂ based instrumentation.

Standard packaging and encapsulation techniques have failed to protect HgI₂ devices for a variety of reasons but the details of the failure mechanisms were not clear. Solving this problem required gaining a better understanding of the mechanisms responsible for device failure and demonstrating that the proper selection of encapsulation technique could significantly improve the operating life of HgI₂. To achieve this, we developed accelerated testing methods and tested a variety of encapsulant types to determine their stability and suitability for use with HgI₂. The chemical, physical, and mechanical properties of the encapsulants were also examined.

The results of this effort include a better understanding of the mechanisms responsible for HgI₂ device failure and their dependence on encapsulant type and a significant increase in crystal stability. This should translate to a potential device life of up to twenty years or more. The significance of these results are far reaching. Stable HgI₂ sensors will not only permit this technology to finally be used in satellite systems but will also provide sensors for many applications. These include room temperature laboratory instruments, portable x-ray fluorescence spectrometers and industrial nuclear gauging equipment.

(NASA-CR-190850) SOFT X RAY WINDOW
ENCAPSULANT FOR HgI₂ DETECTORS
Final Report (Radiation Monitoring
Devices) 62 p

N93-13705

Unclas

Radiation Monitoring Devices, Inc.
44 Hunt Street
Watertown, MA 02172
(617) 926-1167

SOFT X-RAY WINDOW ENCAPSULANT FOR HgI₂ DETECTORS - PHASE II

June 30, 1987

Final Report
Contract NAS 7-931

By:
G. Entine, Ph.D.
K. Shah, M.S.
M. Squillante, Ph.D.

Submitted to:
NASA Resident Office, JPL
4800 Oak Grove Drive
Pasadena, CA 91109

Information on pages 7, 11, 12, 42, 44, 53 and 56 of this report and marked with an asterisk is proprietary. This SBIR data is furnished with SBIR rights under NASA Contract No. NAS 7-931. For a period of 2 years after acceptance of all items to be delivered under this contract the Government agrees to use this data for Government purposes only, and it shall not be disclosed outside the Government during such period without permission of the Contractor. After the aforesaid 2-year period the Government has a royalty-free license to use, and to authorize others use on its behalf, this data for Government purposes, but is relieved of all disclosure prohibitions and assumes no liability for unauthorized use of this data by third parties. This Notice shall be affixed to any reproductions of this data, in whole or in part.

TABLE OF CONTENTS

	PAGE
PROJECT SUMMARY	
COVER PAGE	
TABLE OF CONTENTS	3
I. INTRODUCTION	4
II. CRYSTAL GROWTH	6
A. Crystal Growth Techniques	6
1. EG&G Vapor Transport Process	6
2. Polymer Controlled Growth	7
B. Recipe of PCG Process	9
1. Ampoule Preparation	9
2. Ampoule Loading	9
3. Ampoule Preparation and Crystal Growth	12
C. Device Fabrication	14
III. EVALUATION OF DETECTOR PERFORMANCE	17
A. Electronic Testing Apparatus	17
B. Detector Testing with Low Energy X-Rays	18
C. Estimation of Mobility-Lifetime Products	22
D. Estimation of Energy Required to Produce a Charge Pair	29
E. Variation of Resistance of HgI ₂ Devices with Temperatures	31
F. X-Ray Applications Experiments using HgI ₂ Detectors	33
IV. ENCAPSULATION EXPERIMENTS	37
A. Encapsulant Selection and Characterization	37
1. Copper Diffusion Test	37
2. Permeability Analysis of Encapsulants	38
3. Scanning Electron Microscopy	42
B. Accelerated Testing Under High Temperature and Vacuum	42
1. Theoretical Diffusion Model	42
2. Accelerated Testing	44
3. Comparison of Accelerated Testing to Long Term Testing	45
C. Encapsulant Studies	46
1. Solvent Based Encapsulants	46
2. Parylene Coatings	51
3. Plasma Polymerized Encapsulants	52
V. CONCLUSIONS	58
VI. REFERENCES	61

I. INTRODUCTION

HgI_2 is an excellent semiconductor material for a low energy, room temperature x-ray spectrometer. The high values of the atomic numbers for its constituent elements, 80 for mercury and 53 for iodine, gives high x-ray and gamma ray stopping power. The band gap of HgI_2 is 2.13 eV, which is significantly higher than other commonly used semiconductors (1.12 eV for Si, 0.7 eV for Ge) (1,2). Owing to the large value band gap, the leakage current for HgI_2 devices is smaller, thus allowing low noise performance. In fact, devices fabricated from HgI_2 crystals have demonstrated energy resolution sufficient to distinguish the x-ray emission from the neighboring elements on the periodic table (3-5). Also, the power requirements of HgI_2 are very low. These characteristics make a HgI_2 spectrometer, an ideal component in a satellite based detection system.

Unfortunately, HgI_2 crystals tend to deteriorate with time, even if protected by standard semiconductor encapsulants (6). This degradation ruins the performance of the device in terms of its energy resolution and pulse amplitude. The degrading mechanism is believed to be material loss occurring from below the electrodes, due to high vapor pressure of HgI_2 at room temperature. To address this major obstacle to rapid expansion of HgI_2 technology, we have carried out a research program aimed at improving device stability by encapsulation with inert polymeric materials. The program focused specifically on optimizing the encapsulant materials and their deposition techniques.

The principal objectives for this program were device encapsulation, device testing and accelerated testing to ensure very

long term stability of these high resolution sensors. The crystals used for device fabrication and testing were grown by the Polymer Controlled Growth (PCG), which produced crystals in the form of platelets by vapor transport. In addition, crystals grown by standard vapor transport at EG&G, Santa Barbara and by dimethylsulforide (DMSO) growth process at Laboratoire des Couches et Minces, Algeria, were also investigated.

In view of the low noise characteristics of HgI_2 detectors, the electronic testing set-up was carefully designed and optimized. A specially designed test jig and preamplifier assembly was used for evaluation of detectors. A modified Tennelec 170D preamplifier was used with the front amplification stage incorporated in the test jig. Specially selected components were used for the front end. Stray capacitance was reduced as much as possible. In this manner, the electronic noise contribution from the preamplifier was reduced to 320 eV FWHM as measured by using a pulser.

A variety of encapsulants were investigated with the selection criteria based on their chemical diffusion barrier properties, mechanical stability, reactivity and morphology of encapsulant films. The investigation covered different classes of encapsulants including solvent based encapsulants, vapor deposited encapsulants, and plasma polymerized encapsulants. A variety of characterization techniques were employed to examine their effectiveness in stabilizing HgI_2 devices; these included permeability evaluation, vacuum and heat testing, scanning electron microscopy (SEM) as well as studying the detector performance of coated detectors. The results of all these experiments increased our understanding of the problem and the plasma polymerized

films appear to have entirely solved the HgI₂ degradation problem. Another major achievement of this program was the development of an accelerated testing technique which correlates extremely well with long term testing.

II. CRYSTAL GROWTH.

A. Crystal Growth Techniques - The techniques available for the growth of HgI₂ crystals are limited by the fact that a crystallographic phase change occurs at approximately 127°C (7). Above this temperature, the red tetragonal room temperature phase changes reversibly into the yellow orthorhombic phase. This phase transformation makes it impossible to grow HgI₂ from melt despite the relatively low melting point of 250°C. Hence the standard crystal growth techniques for semiconductors, like Bridgman or Chochralski which start from a melt, are ruled out.

Solution growth techniques using various organic solvents have produced crystals of sufficient size but of consistently inferior electrical quality (8,9). Vapor grown techniques have so far produced crystals having the best electrical characteristics. Among the the vapor growth techniques, slow vapor transport with precise temperature control and Polymer Controlled Growth (PCG) have shown the most promise.

1. EG&G Vapor Transport Process - This technique of crystal growth, which stems from the Temperature Oscillation Method originally developed by Scholz (10), is a vapor phase growth process with a small temperature gradient between the source material and the growing crystal. This technique is slow but is capable of producing large

crystals of HgI_2 weighing 700g or more. Since little or no purification occurs during the growth stage, this process must be preceded by suitable purification process. At the present time this is done by a combination of vacuum casting of the virgin powder followed by a time consuming multiple distillation process. In spite of these efforts, various analytical techniques such as SIMS reveal the presence of numerous impurities like lithium, carbon, sodium, magnesium, aluminum, silicon, potassium, calcium, titanium and iron and in concentration greater than parts per million.

2. Polymer Controlled Growth - The PCG crystal growth method is closed tube vapor transport technique invented at Purdue University by Dr. S. Faile. It is very different from previous vapor growth techniques because of the addition of an organic polymer to the starting material for growth (10). The process is operationally easy as well as fast and has enjoyed very good success. The polymer appears to contribute to both material purification and platelet formation.

The basic PCG crystal growth process simply involves sealing research grade HgI_2 (99.999%) in a quartz ampoule with 1% by weight of a polymeric material such as styrene or polyethylene. Vapor transport is then initiated by heating one end of the ampoule to 230°C while the other end is below 127°C . The resulting crystals are formed by vapor transport in the form of thin platelets, up to 200 microns thick and often reaching areas in excess of 1cm^2 . The entire process is completed in about 3 days. Figure 1 shows a schematic of a PCG furnace.

The PCG process was used to grow crystals in the current program due to improved material purity, ease of operation and faster

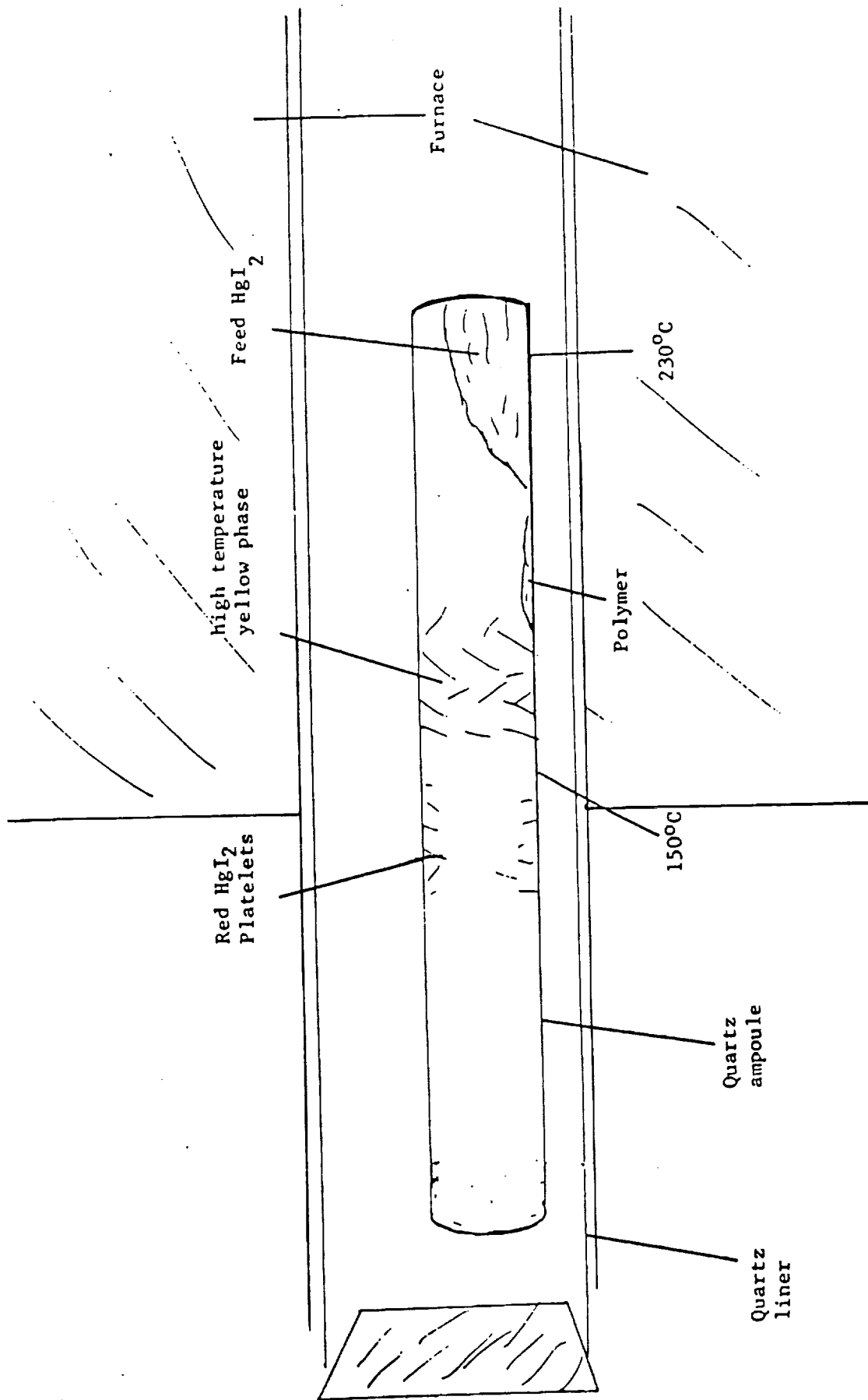


FIGURE 1
Schematic of typical ampoule in furnace during growth of HgI_2 platelets.

production. The EG&G process does have an advantage over PCG in terms of more control over crystal size and shape.

B. Recipe of PCG Process - During the early part of the program, we fabricated devices on crystals grown several years ago during a previous research program. However the yield of successful devices from these crystals decreased as the better crystals were used up. This situation necessitated growth of more HgI_2 crystals.

Facilities needed for crystal growth of HgI_2 by the Polymer Controlled Growth process were set up including two furnaces specially designed for HgI_2 crystal growth. Figure 2 shows a photograph of one of the furnaces. These furnaces were hooked up to dual temperature controllers providing an optimal temperature profile for crystal growth. Figure 3 shows such a temperature profile. Maintaining a proper temperature profile is essential since it greatly influences the dynamics of crystal growth. Various steps followed during crystal growth process are discussed below.

1. Ampoule Preparation - In order to grow pure HgI_2 crystals, utmost care was taken during ampoule preparation. Research grade quartz was used throughout. The open ended quartz tube was cut to about 10-12 inches and one of its ends was sealed. A dimple was made about 4 inches at the other end, which served as a resting point for a sealing plug. An appropriate quartz plug was prepared. The ampoule and plug were sequentially washed with concentrated HNO_3 , deionized water and acetone. The ampoule was then evacuated (to less than 50 microns Hg) and flushed with argon to remove final traces of any solvents left behind.

2. Ampoule Loading - The next step was loading the ampoule

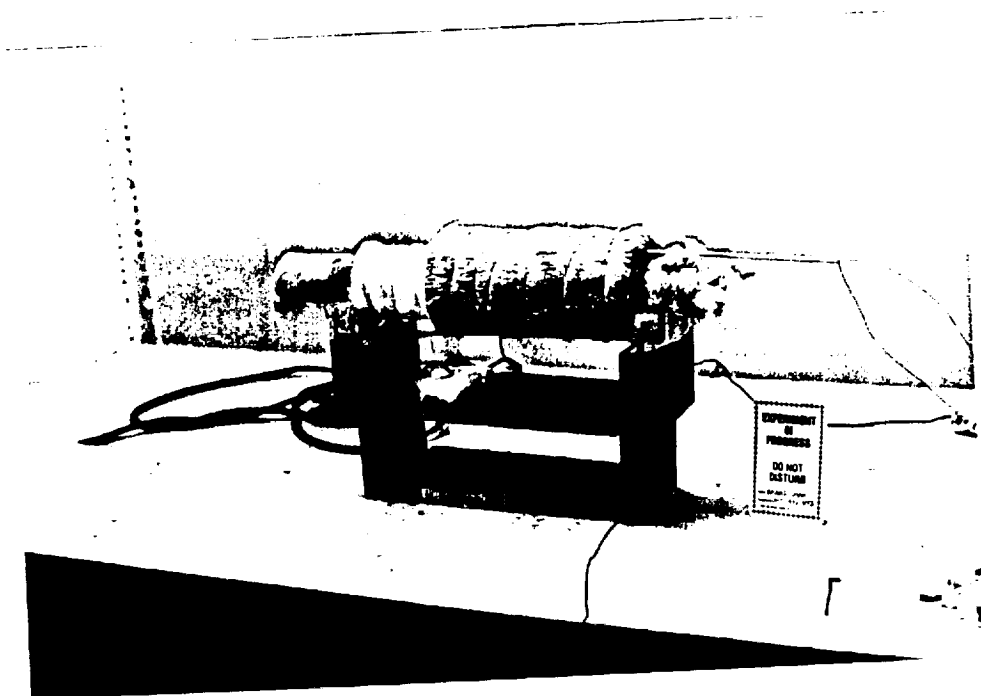


FIGURE 2
Furnace used for Crystal Growth of Mercuric Iodide
By PCG Method

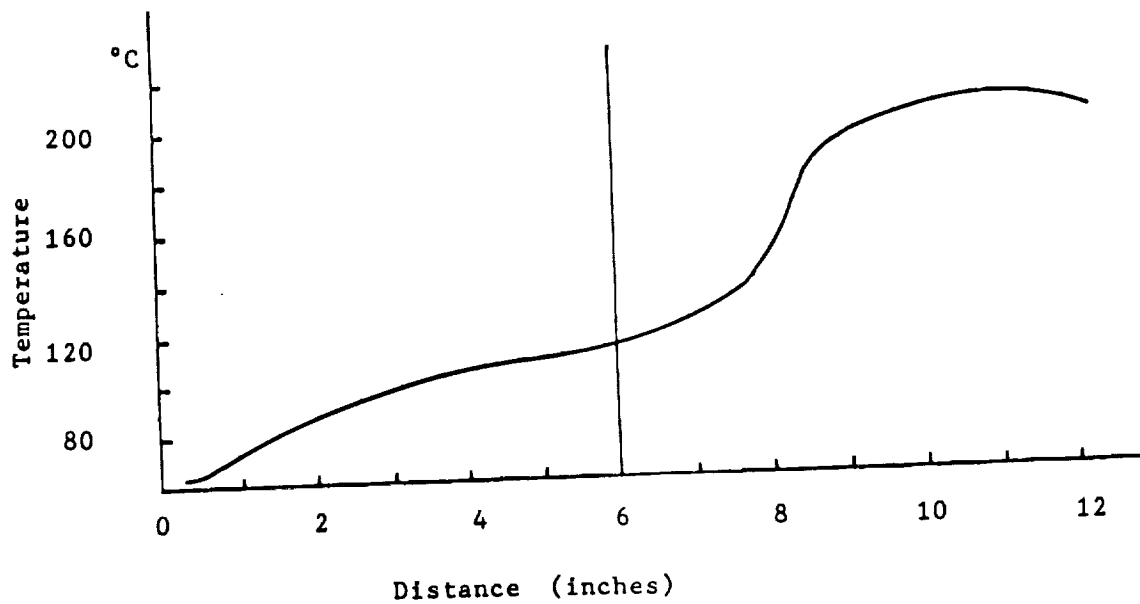
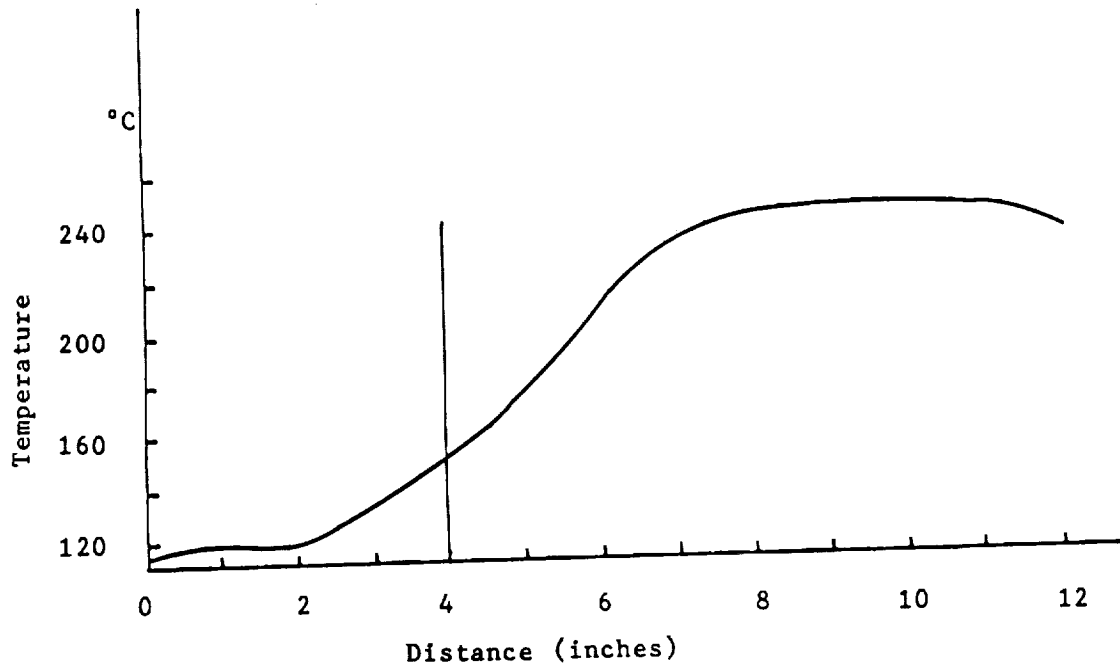


FIGURE 3

Temperature Profiles for Crystal Growth Furnaces

Upper Figure: Flipping Furnace Lower Figure: Crystal Growth Furnace

with HgI_2 powder (SPEX research grade-99.999%) and polyethylene as a transporting agent (1% by weight). The polymer was cut into pieces about 1cm^2 before loading. The filled ampoule was then evacuated, back filled with argon and re-evacuated. It was finally sealed using a plug at a pressure of less than 50 microns Hg. Figure 4 shows a schematic of an ampoule. *

3. Ampoule Preparation and Crystal Growth - The ampoules were prepared for crystal growth using a technique termed "flipping". Flipping is the process of transporting the material back and forth in the ampoule by vapor transport process. The purpose of this operation is to ensure proper mixing of mercuric iodide powder with the polymeric transporting agent.

During flipping the source end of the ampoule containing the material was inserted into the furnace maintained at 250° . This caused the material to transport rapidly to the opposite end maintained at ambient temperature. The ampoule was then reversed and the process was repeated, so as to return all the material to the source side. This completed one flipping process which took about 6 hours. Ampoules were usually "flipped" twice.

A crystal growth was carried out in a specially designed two zone furnace. The source region was maintained at 230° while the growth region being controlled at 115°C . Growth runs were completed in about 2 days.

The platelets selected from the growth runs for detector fabrication appeared smooth and clear without any pits or ridges on the surface. This was considered essential since previous experience *

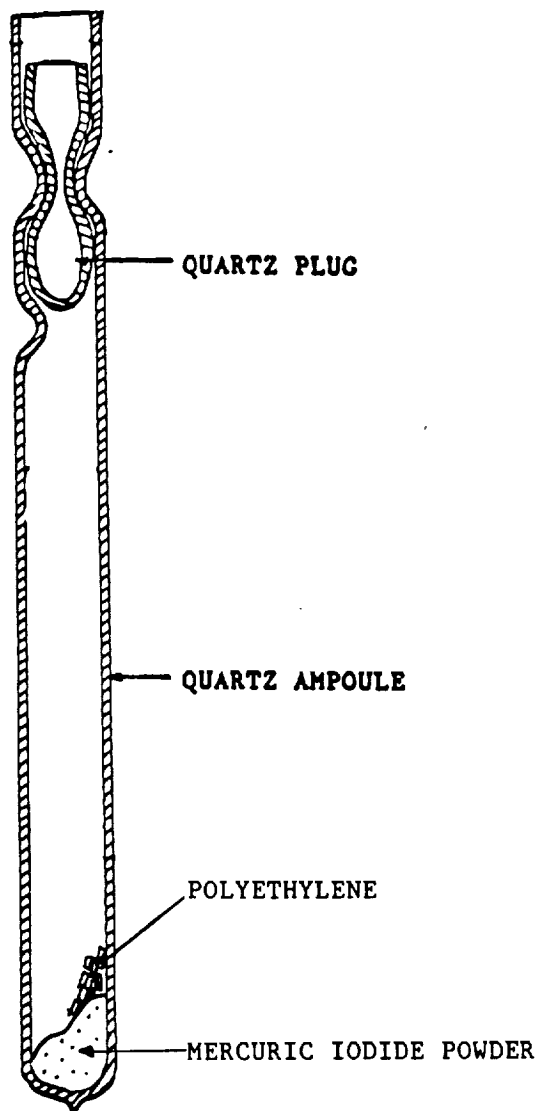


FIGURE 4
Schematic of the Growth Ampoule

indicated that smooth, clear crystals made better detectors.

C. Device Fabrication - The device fabrication technique was developed in conjunction with the University of Southern California. The primary concern is the extreme fragility of Hg_2 crystals. It is for this reason that NASA has been attempting to grow large HgI_2 crystals in free fall as a part of its space shuttle program.

The mechanical properties of HgI_2 are a direct consequence of the layered structure of HgI_2 , where each I-Hg-I layer lies normal to the tetragonal Z axis and provides easy cleavage along (001) axis. Figure 5 shows the crystal structure of HgI_2 . In view of the fragile nature of HgI_2 crystals, the necessary handling of crystals during their removal from the growth ampoule and deposition of contacts was approached with maximum care. The crystals were usually supported on small slips of paper and moved around by gently tapping the paper with a finger. The electrical contacts were formed by applying a layer of Eccocoat diluted with n-butylacetate using a fine camel hair brush. A 25 micron palladium wire was used to connect the device to the test electronics. The wires were anchored to a ceramic substrate using a Dow Corning RTV to reduce mechanical strain during testing. Figure 6 shows a sketch of the device structure. This procedure worked very well when PCG crystals were used and no surface treatment or cleaning was found necessary.

In the case of EG&G grown material, the crystals were in the form of a cube about $1cm^3$ in volume. To make devices these crystals were cleaved along a plane perpendicular to the C axis. This was done by using a razor blade; the block was separated into slices about 1 mm thick. In order to remove the surface damage caused by cleavage, the

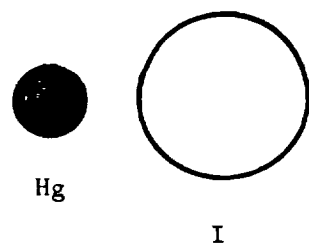
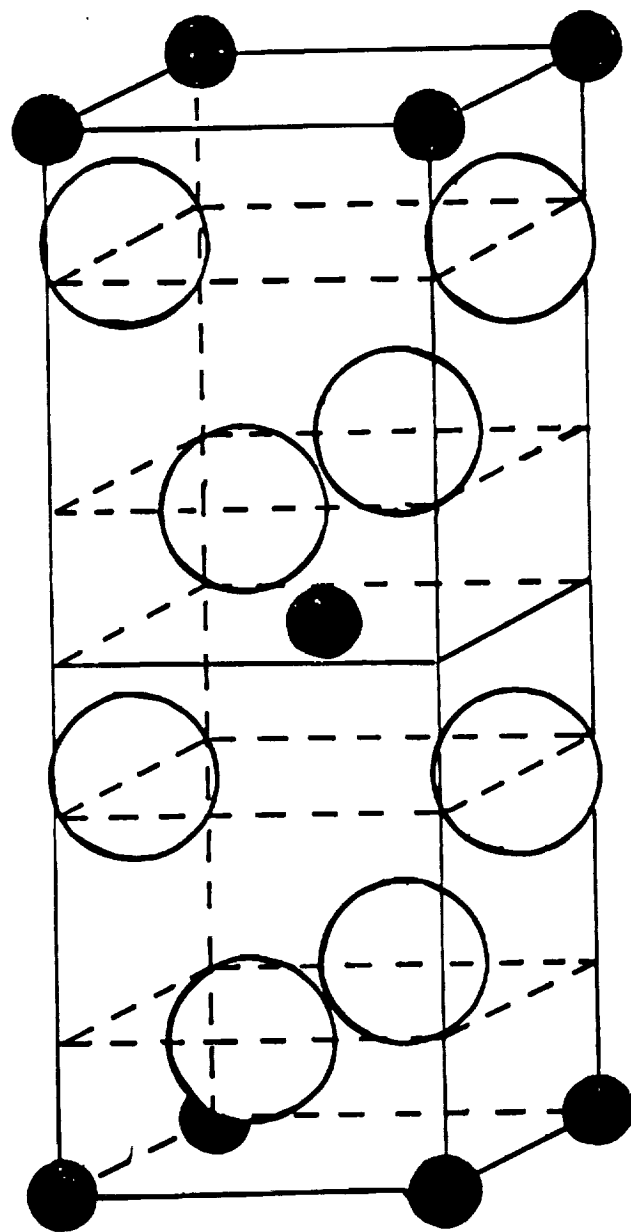


FIGURE 5

Crystal Structure of $\alpha\text{-HgI}_2$

$a = 4.361 \text{ \AA}$, $c = 12.45 \text{ \AA}$

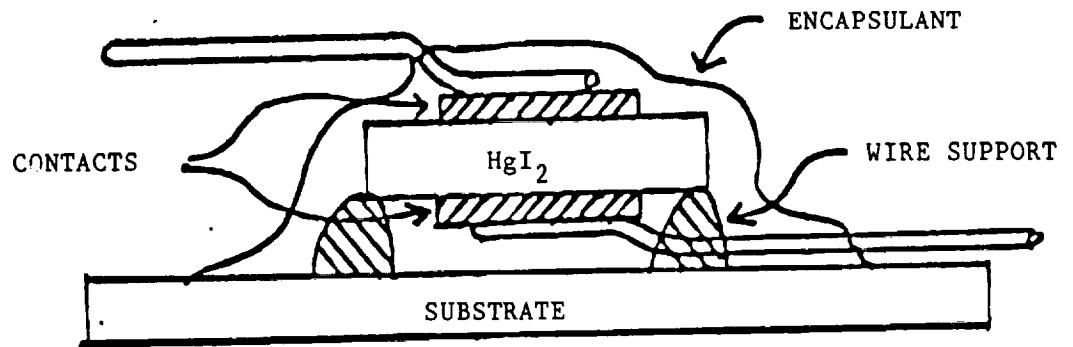


FIGURE 6
A Sketch of the HgI_2 Device Structure

crystals were etched using 20% potassium iodide (KI) solution. The crystals were washed with distilled H₂O, and allowed to dry. The resulting final thicknesses varied between 250 and 500 microns. Device fabrication was carried out using the same procedure as in the case of PCG platelets.

In the case of solution grown crystals, the crystals were about 2 cm² and about 0.5cm thick. These crystals were also cleaved using the procedure described above. In addition to the KI etch, we tried a dilute acid etch, which was recommended by Dr. Mohammed Brahim. However the device performance degraded when the acid etch was used and hence the treatment was abandoned.

The crystals grown by PCG and the EG&G process appeared bright and shiny while the ones grown from solution appeared to be dull and flaky suggesting inferior properties. Upon device testing the PCG and EG&G crystals operated with much lower noise than the solution grown ones.

III. EVALUATION OF DETECTOR PERFORMANCE

A. Electronic Testing Apparatus - The apparatus used to test the devices consisted mainly of standard nuclear electronic instrumentation. However, the test jig and preamplifier were specially designed in view of ultra low noise characteristics of HgI₂ devices.

At the beginning of the program, the testing of detector performance was carried out in a standard electronic instrument housing with a removable cover which provided a light tight seal. Inside the box were mounted a preamplifier (Polish type 1002, PO-721) and a stage for mounting the HgI₂ detectors. This apparatus sufficed to evaluate gross

detector performance, but the preamplifier noise above 1 keV limited sensitivity of measurements.

The noise remained persistent in spite of our efforts and hence we decided to replace the preamplifier and redesign the test jig based on a design provided to us by JPL. In order to meet this objective, noise characteristics of two low noise preamplifiers, Tennelec Model 170D and Canberra model 2001, were investigated. Upon detailed evaluation, the noise contribution of Tennelec 170D was found to be 650 eV (FWHM-pulser) while it was 1 keV (FWHM-pulser) for Canberra 2001. Hence, Tennelec 170D preamplifier was selected.

The Tennelec preamplifier was modified to better match the characteristics of the low capacitance, high resistivity HgI_2 devices. It was positioned next to a vacuum test chamber with the front end of the preamplifier mounted inside the jig. For this front stage of amplification, hand selected low noise components were used, which included a low noise decapsulated FET (2N4416) and 5 G ohm feedback resistor. The test jig was connected to the preamplifier through specially provided feed throughs. The stray capacitance was reduced as much as possible in the test apparatus. The basic preamplification noise contribution was thus reduced to 320 eV (FWHM-pulser) at room temperature. The output from the preamplifier was fed into an ORTEC 410 NIM linear amplifier. The output was observed on an oscilloscope and the spectrum was recorded on a Norland model 5400 MCA. A transistor power supply Model 212A manufactured by Electronic Measurements Company was used to provide detector bias.

B. Detector Testing with Low Energy X-rays - The detector to be

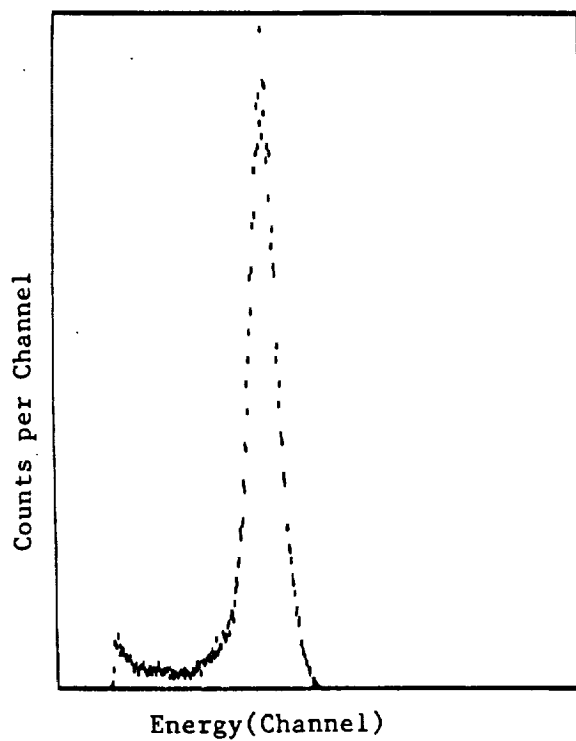
tested was mounted on a stage positioned in the center of the test jig. The ^{55}Fe x-ray source was mounted directly above the detector on the inner wall of the vacuum chamber. The bottom lead from the device was connected to the gate of the input FET and the top lead to the negative bias line. The 5.9 keV X-rays from the ^{55}Fe source are stopped within the top few microns of HgI_2 , hence the holes generated during the interaction of X-rays with HgI_2 have to travel a very small distance to reach the top negative electrode, while the electrons travel through the bulk of the device to reach the positive electrode. Since the electrical transport properties of the electrons are superior to those for holes, such an arrangement provided best results in terms of energy resolution. The connections were kept clean and an electronic grade solder was used to make connections in order to obtain low noise performance. A 5 microseconds shaping time was found to give best results. On testing the detector bias was increased gradually until the noise was seen to increase significantly.

Table I lists the performance characteristics of some of the detectors fabricated. It can be seen from the table that both the PCG and EG&G crystals were found to exhibit similar performance characteristics. It can be also noticed that a correlation exists between the leakage current of the device and its energy resolution. The best energy resolution was found to be 480 eV (FWHM-5.9 keV X-rays) for an EG&G crystal and 500 eV (FWHM-5.9 keV X-rays) for a PCG crystal. Figure 7 shows these spectra.

Various means were employed to improve detector performance. Extreme care was taken during the detector fabrication stage to be sure

TABLE I

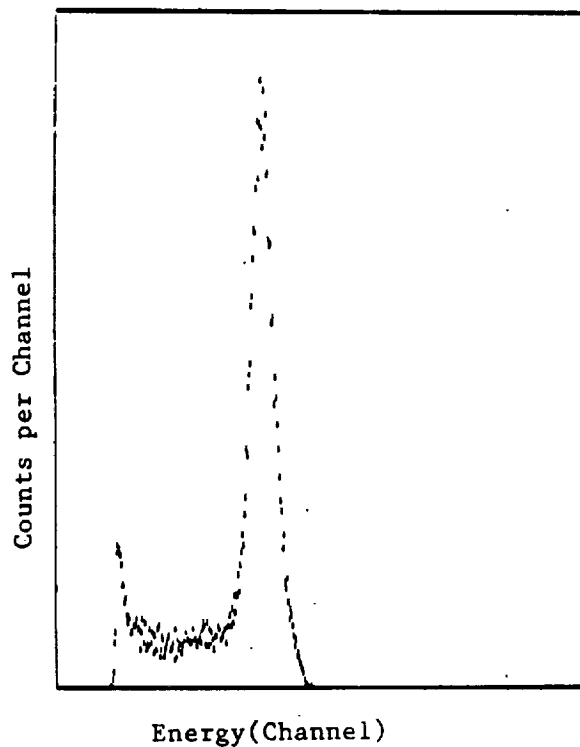
Detector #	Crystal Type	Bias	Peak Position	FWHM	I_L	P/V
UC-1	PCG	-15V	160	500eV	7pA	13
UC-2	PCG	-100V	159	650eV	12pA	5.54
UC-3	PCG	-120V	157	650eV	15pA	4
UC-4	EG&G	-20V	153	480eV	5pA	12
UC-5	EG&G	-60V	159	600eV	10pA	10
UC-6	EG&G	-20V	162	550eV	8pA	6.5
UC-7	EG&G	-50V	156	510eV	4pA	15



Source: Fe⁵⁵

Resolution: 480 eV
(FWHM)

Crystal Type: EG&G



Source: Fe⁵⁵

Resolution: 500 eV
(FWHM)

Crystal Type: PCG

FIGURE 7

Fe⁵⁵ (5.9 KeV X-rays) Spectra Measured with HgI₂ Detectors

that the two electrodes were exactly above one another. If there is any offset in this arrangement, the regions not coinciding cause the formation of electronic fringe fields. This degrades the low energy side of the photopeak. In such a case, the spectrum could be improved by adding a collimator to the device made of Dow Corning RTV. Figure 8 shows such an arrangement.

Detector capacitance affected device performance. Since the detector capacitance is directly proportional to the active area and inversely proportional to the detector thickness, the reduction of the capacitance could be brought about either by decreasing the area of the contacts or increasing the thickness of the detector. Reducing the detector area decreases the detection efficiency, while increasing the detector thickness necessitates much higher detector bias and reduces the charge collection efficiency.

Additional improvement was almost invariably achieved by cooling the detector and the associated electronics as shown in Figure 9.

C. Estimation of Mobility-Lifetime Products - In addition to recording the pulse height spectra produced with HgI₂ detectors, experiments were also conducted to evaluate the charge carrier transport properties of HgI₂ crystals. These experiments helped in material characterization and served as a basis for comparing the crystals grown by the two processes.

Standard analysis using the Hecht theory was used to evaluate the mobility-lifetime ($\mu\tau$) product (12). The experiments involved measuring the position of the photopeak for 5.9 keV x-rays from an ⁵⁵Fe source as a function of the detector bias. In theory, the photopeak position

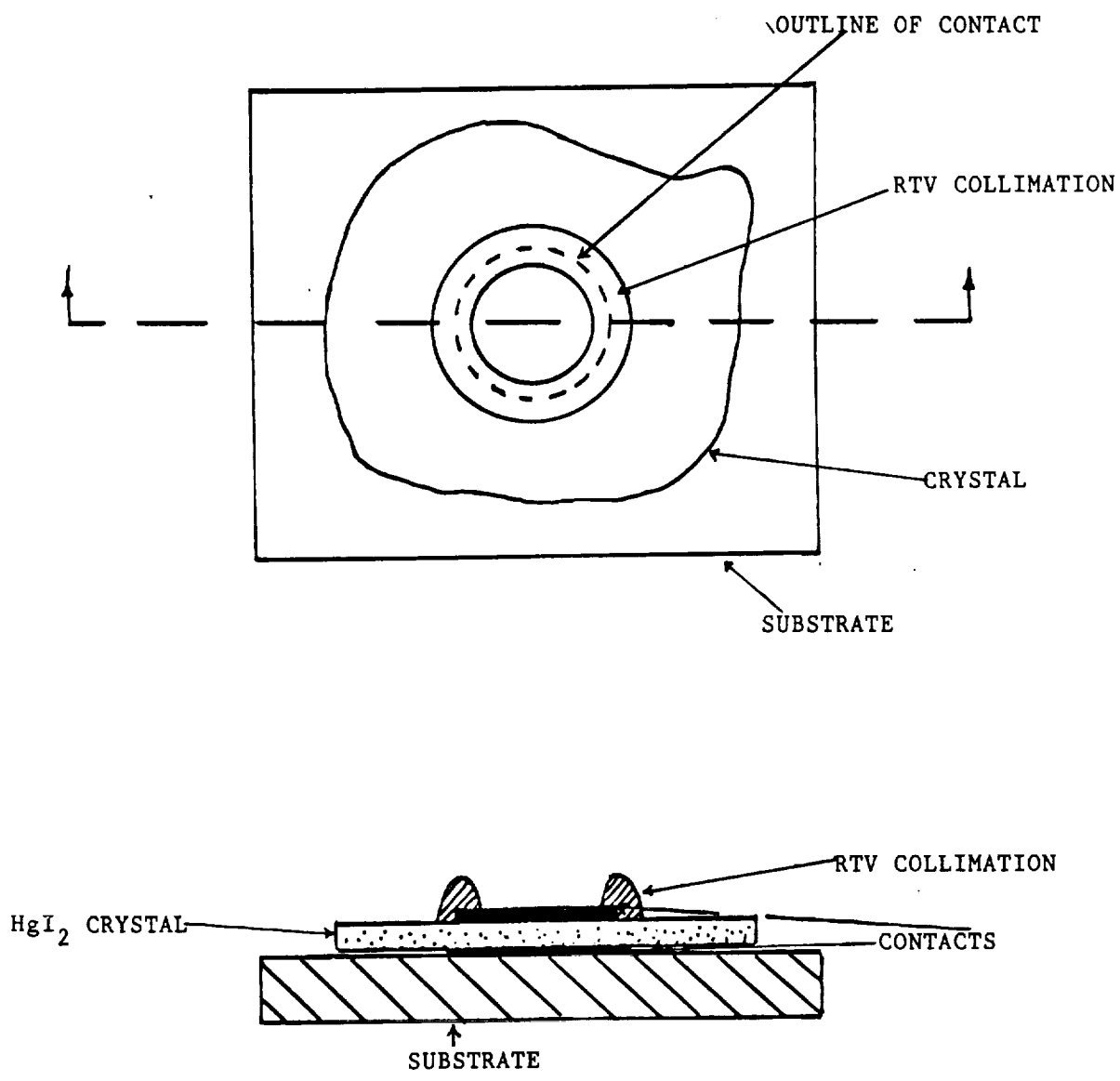
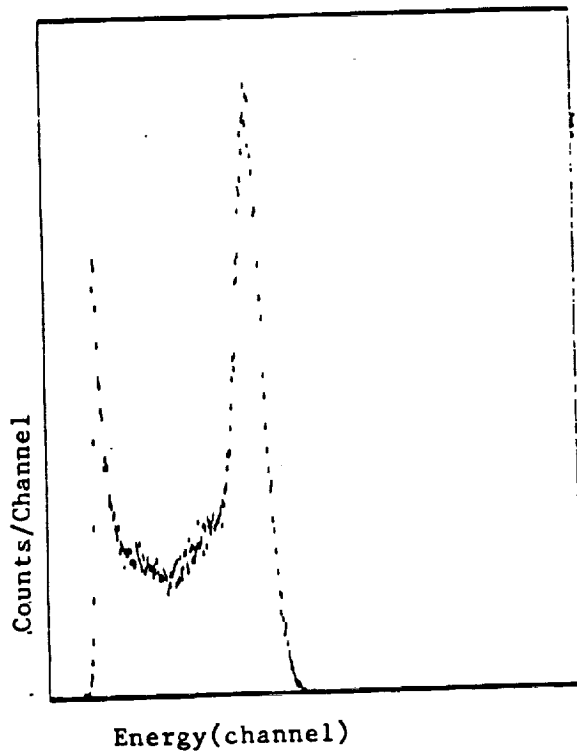
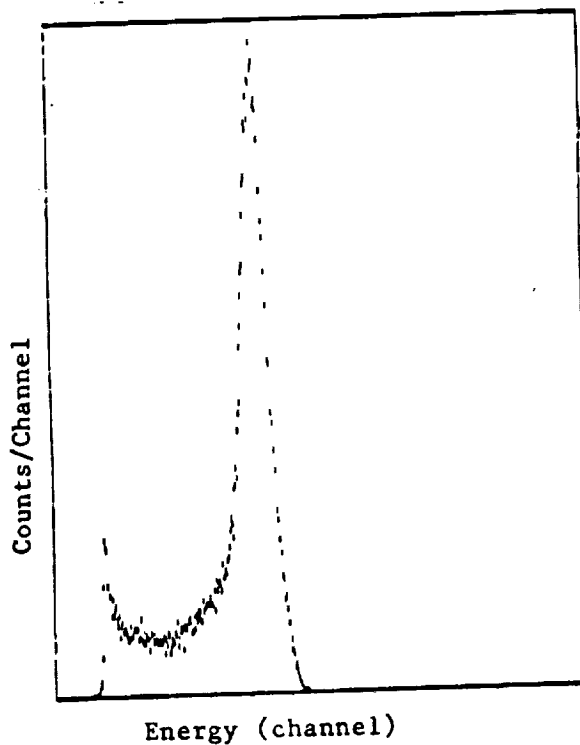


FIGURE 8

Schematic of Device Collimation Using Dow-Corning RTV



Source: Fe^{55}
Temperature: 25° C
FWHM: 600 ev



Source : Fe^{55}
Temperature: -10° C
FWHM: 520 ev

FIGURE 9
Effect of Operating Temperature on
Detector Performance

should increase as the bias increases and eventually reach a position which does not change with bias. This situation would indicate 100% charge collection efficiency. The Hecht relationship can be expressed as follows:

$$n = a\{1 - \exp(-l/a)\} \quad (1)$$

where n = charge collection efficiency, a = drift length $= \mu\tau V/d^2$, $\mu\tau$ = mobility-lifetime product for electrons, V = detector bias, and d = detector thickness.

Equation 1 correctly predicts the mobility-lifetime product in case of alpha-particles or low energy x-rays where the interaction occurs almost entirely at the top surface. The variation of the peak position as a function of negative bias applied to the top contact was recorded and the mobility-lifetime product of electrons computed. Figure 10 shows experimental results for negative bias for a EG&G and a PCG crystal. By inverting the polarity of the bias, the hole transport properties were investigated. Figure 11 shows these experimental results. Table II records the experimental parameters and lists the computed mobility-lifetime product. It should be noted that a parametric fit of Equation 1 was utilized with the experimental data to calculate the required mobility-lifetime product.

As can be seen in Table II, the mobility-lifetime product of electrons for both EG&G and PCG crystals is about 2×10^{-4} cm²/volt which confirms the similarity of these materials. The mobility-lifetime product of holes was computed to be 1.6×10^{-5} cm²/volt for PCG crystals which is among the highest recorded to date.

The accurate estimation of detector thickness is essential in

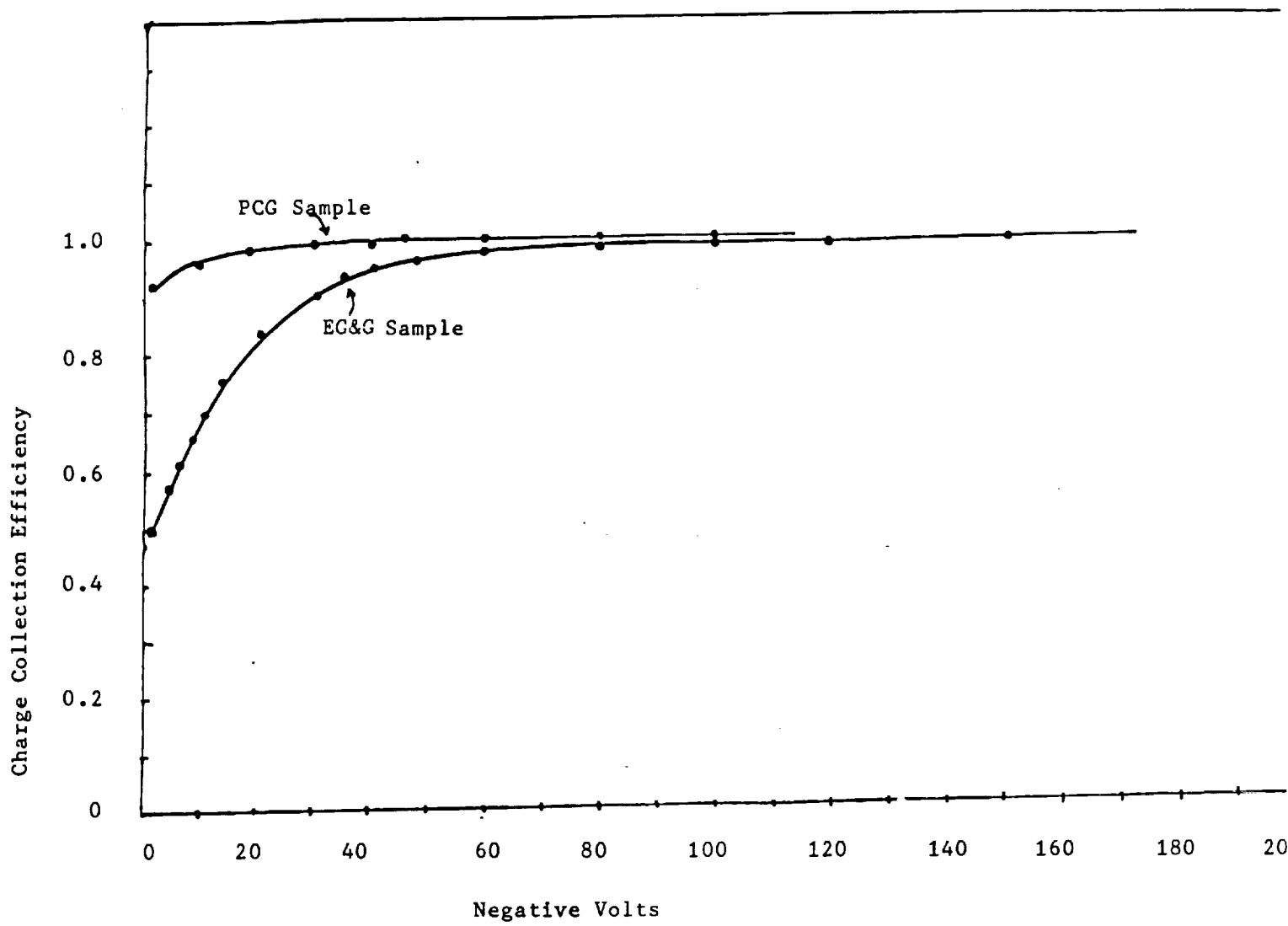


FIGURE 10

Variation of Charge Collection Efficiency with Negative Bias

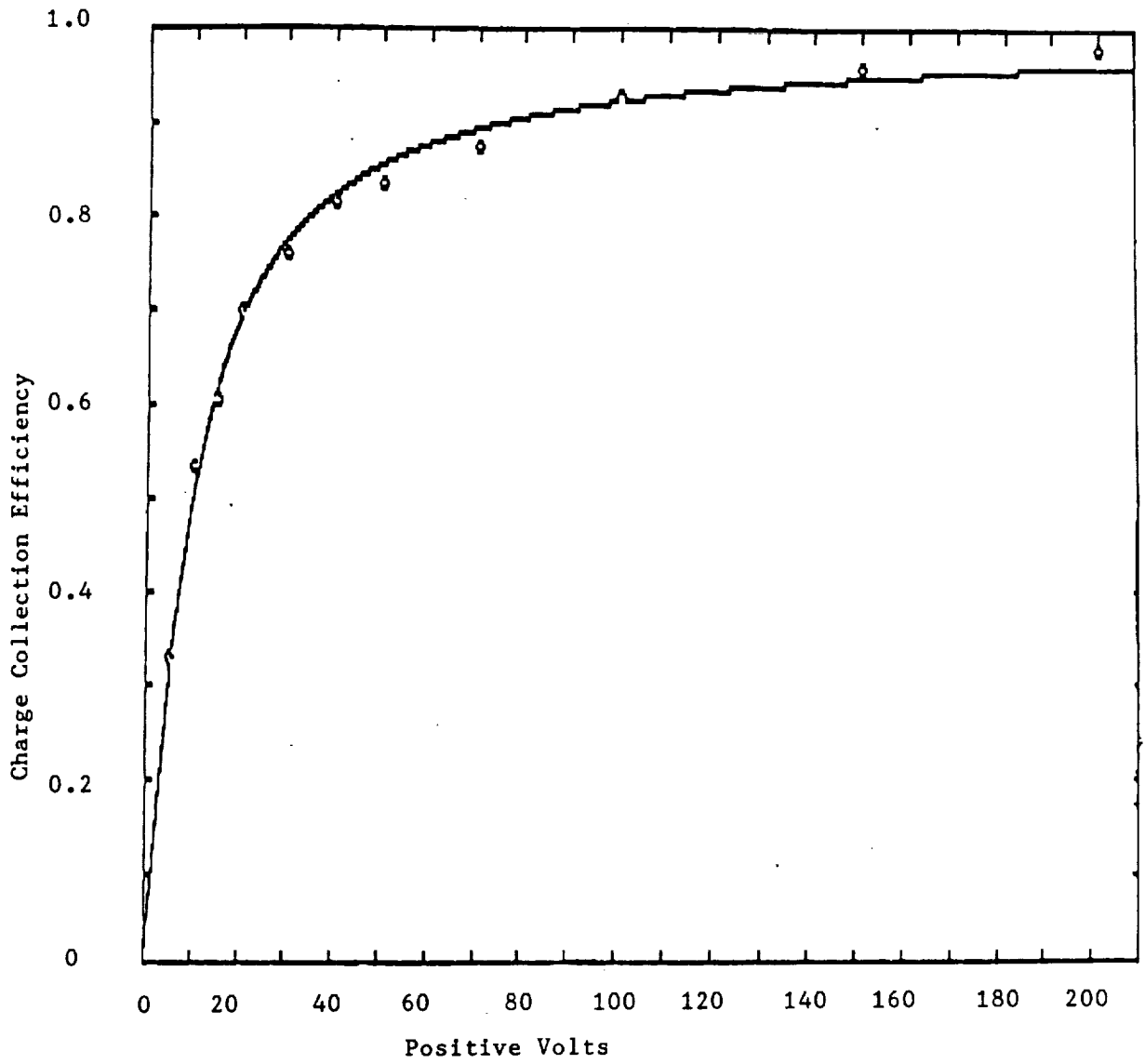


FIGURE 11
Variation of Charge Collection Efficiency with Positive Bias

TABLE II
Mobility-Lifetime Product for Charge Carriers

No.	Crystal Type	Polarity of Bias	Thickness of Detector(microns)	Mobility-Lifetime cm^2/volt
1	PCG	-	100	2.4×10^{-4} (electron)
2	EC&G	-	270	2.2×10^{-4} (electron)
3	PCG	+	150	1.6×10^{-5} (holes)

precise computation of mobility-lifetime products. It was measured using both by weighing the crystals and x-ray attenuation.

D. Estimation of Energy Required to Produce a Charge Pair - The magnitude of the signal produced from a semiconductor sensor is inversely proportional to the incident energy required to generate a charge pair, E_{pair} . In most semiconductors this energy is roughly three times the energy of the band gap, E_g . For example, E_g for silicon is 1.1 eV and the energy required to produce a charge pair is 3.10 eV (1).

Reported values of E_{pair} for HgI_2 are anomalously low. This gives HgI_2 an inherent advantage relative to other semiconductors. The large band gap semiconductors have the advantage of lower leakage current and hence lower noise contribution, the larger band gap however also results in a lower signal because of the greater energy required to produce a charge pair.

Experiments were conducted to measure E_{pair} in our HgI_2 devices. Figure 12 shows a plot of E_{pair} vs E_g for many semiconductors. It can be seen from the figure that a linear relationship can be fitted between these two parameters for many semiconductors. However, for HgI_2 with $E_g = 2.13$ eV, the predicted value of E_{pair} from the relation in the figure is 6.5 eV which is significantly higher than the literature value of 4.5 eV. In order to confirm this data, we performed an experiment to estimate E_{pair} for HgI_2 . It involved energy calibration of the multi-channel analyzer using a CdTe detector operated near 100% efficiency using the 60 keV photopeak from an Am^{241} source as reference. Next the CdTe detector was replaced by an HgI_2 detector and the Am^{241} spectrum produced by this detector was recorded. From the ratio of the

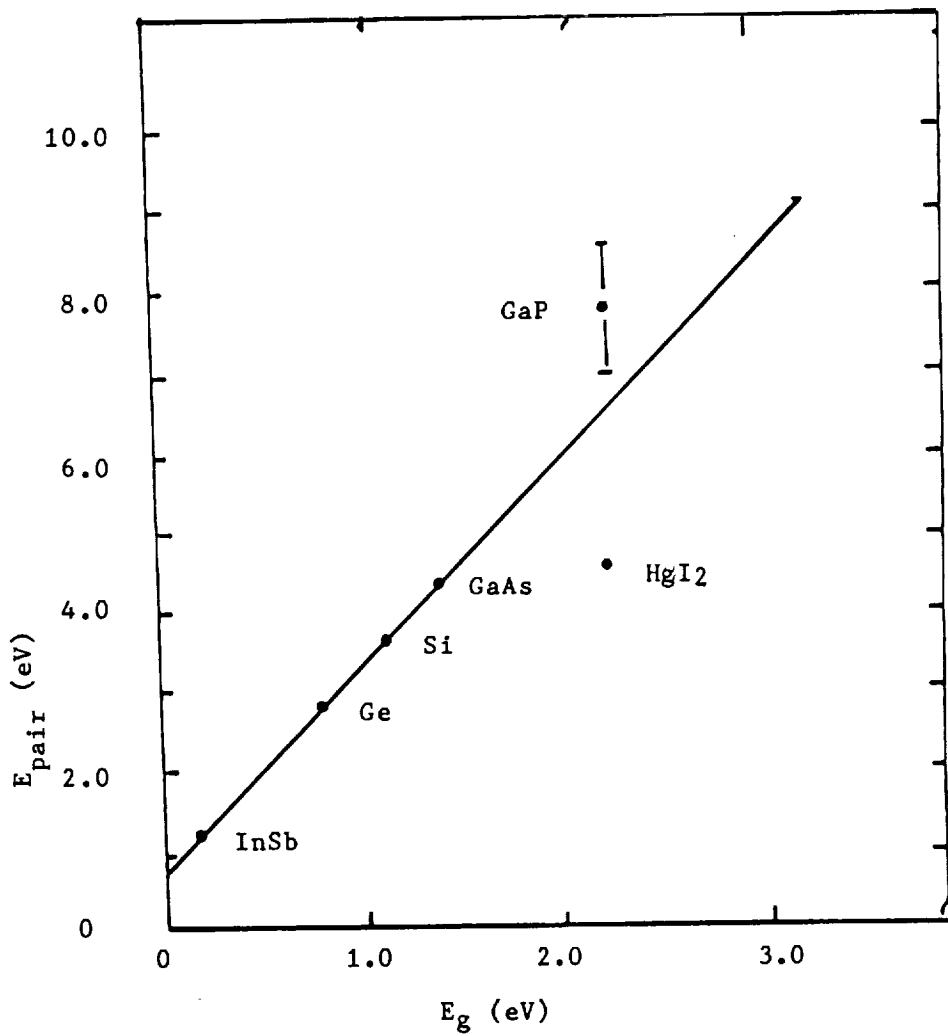


FIGURE 12

Variation of E_{pair} with E_g for Different Semiconductors

peak position for the 60 keV photopeak for CdTe and HgI₂ detectors, and knowing the value of E_{pair} for CdTe to be 4.4 eV, the value of E_{pair} for HgI₂ was determined to be 4.5 eV. Table III lists the experimental results.

E. Variation of Resistance of HgI₂ Devices with Temperature - This experiment constituted a standard characterization experiment for semiconductors, with the aim of identifying trapping levels in the band gap due to impurities. In the absence of impurities, the band gap could be evaluated. The charge carrier concentration due to thermal ionization can be expressed as follows (13):

$$n_i = (N_c N_v)^{1/2} \exp(-E_g / 2kT) \quad (2)$$

where

n_i is the intrinsic concentration of free electrons

N_c is the effective density of states in the conduction band

N_v is the effective density of states in the balance band

E_g is the band gap

K is Boltzman's constant

T is absolute temperature

An experiment was conducted to measure the dark leakage current of a HgI₂ sample as a function of the absolute temperature. The temperature of the sample was varied to from 25°C to -35°C, and the dark leakage current was measured using a Keithley electrometer. For a relatively small temperature variation as in the present case, the temperature dependence of N_c and N_v can be neglected. Thus the leakage current can

TABLE III

Detector Type	Source/Energy	Bias	Peak Position 60keV	Detector Capacitance	eV/pair
CdTe	$\text{Am}^{241}/60\text{keV}$	150V	436	3pF	4.4 (from literature)
HgI ₂	$\text{Am}^{241}/60\text{keV}$	300V	420	3pF	4.5 (calculated)

be related to temperature using a simple exponential. Figure 13 shows a plot of variation of logarithm of leakage current with the inverse of temperature (absolute). As expected from Equation 2, the data on the plot presents a linear relationship. From the slope of the line, the band gap was computed to be 2.15 eV.

This measurement was made on a PCG crystal. The analysis indicates that the PCG process produces pure crystals because small amounts of impurities (few parts per million) would distort the relationship given by Equation 2 at the temperatures studied and in such a case the analysis would yield the impurity level in the band gap.

F. X-Ray Applications Experiments using HgI₂ Detectors - A simple demonstration experiment was performed using HgI₂ detectors for x-ray fluorescence analysis using an isotopic excitation source. The good energy resolution of HgI₂ detectors along with small size, low power consumption and negligible cooling requirements make them a very attractive candidate for field portable x-ray fluorescence systems as well as space borne systems.

The experiment involved bombarding a titanium foil (about 2 mm thick) with 5.9 keV x-rays from an ⁵⁵Fe source. The resulting x-rays emanated from titanium corresponding to the K-shell transition have energy of 4.5 keV and were directed onto a HgI₂ detector. Figure 14 shows the resulting energy spectrum produced. The principal peak corresponds to the 4.5 keV K x-rays from titanium, and the smaller peak on the higher energy side corresponds to the backscattered photons from ⁵⁵Fe (5.9 keV).

In another experiment, a HgI₂ detector was utilized to determine

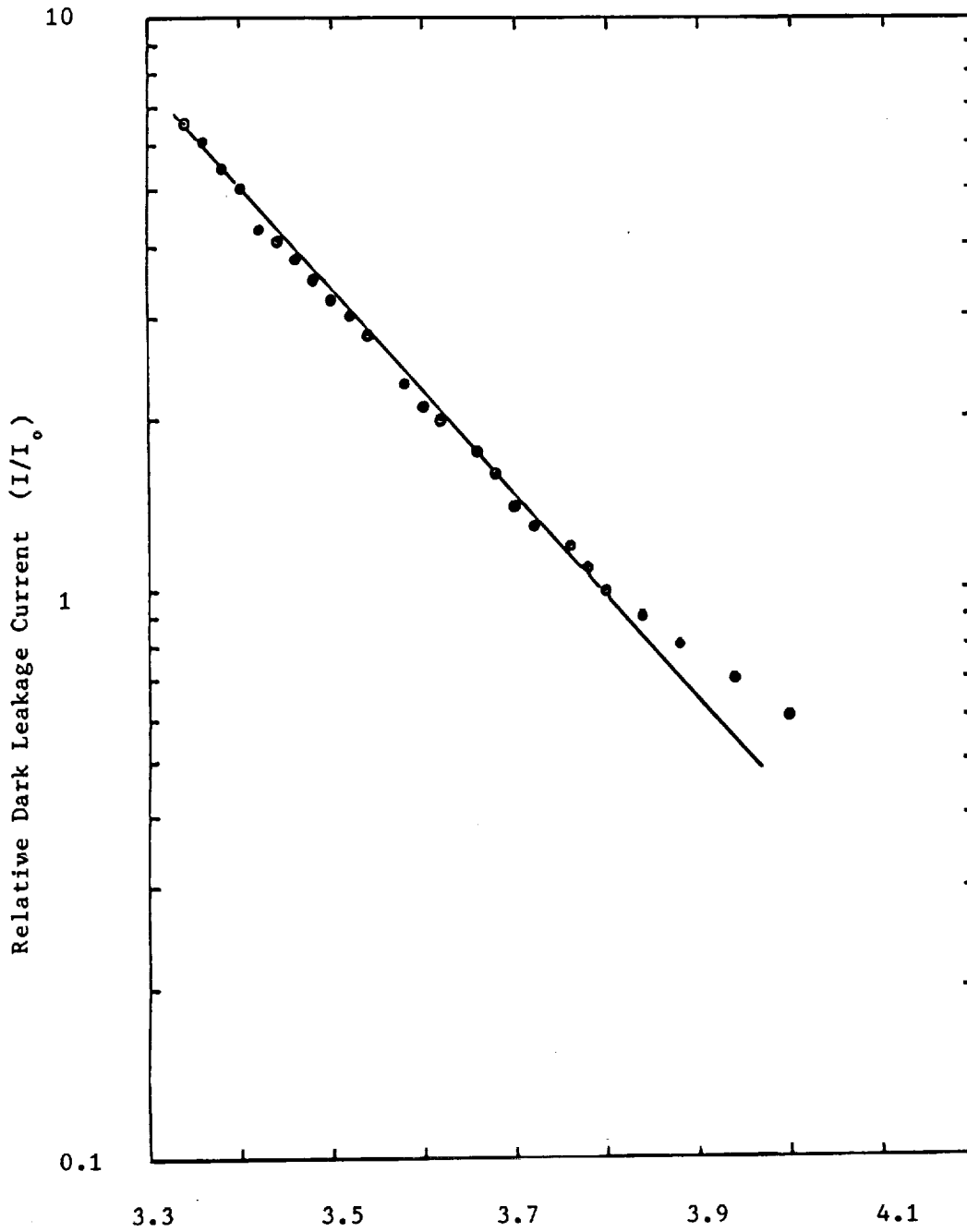


FIGURE 13

Relative Dark Leakage Current as a Function of Reciprocal Absolute Temperature for a HgI_2 Sample. The Slope of the Solid Line Corresponds to the Band Gap of HgI_2 (2.15 eV)

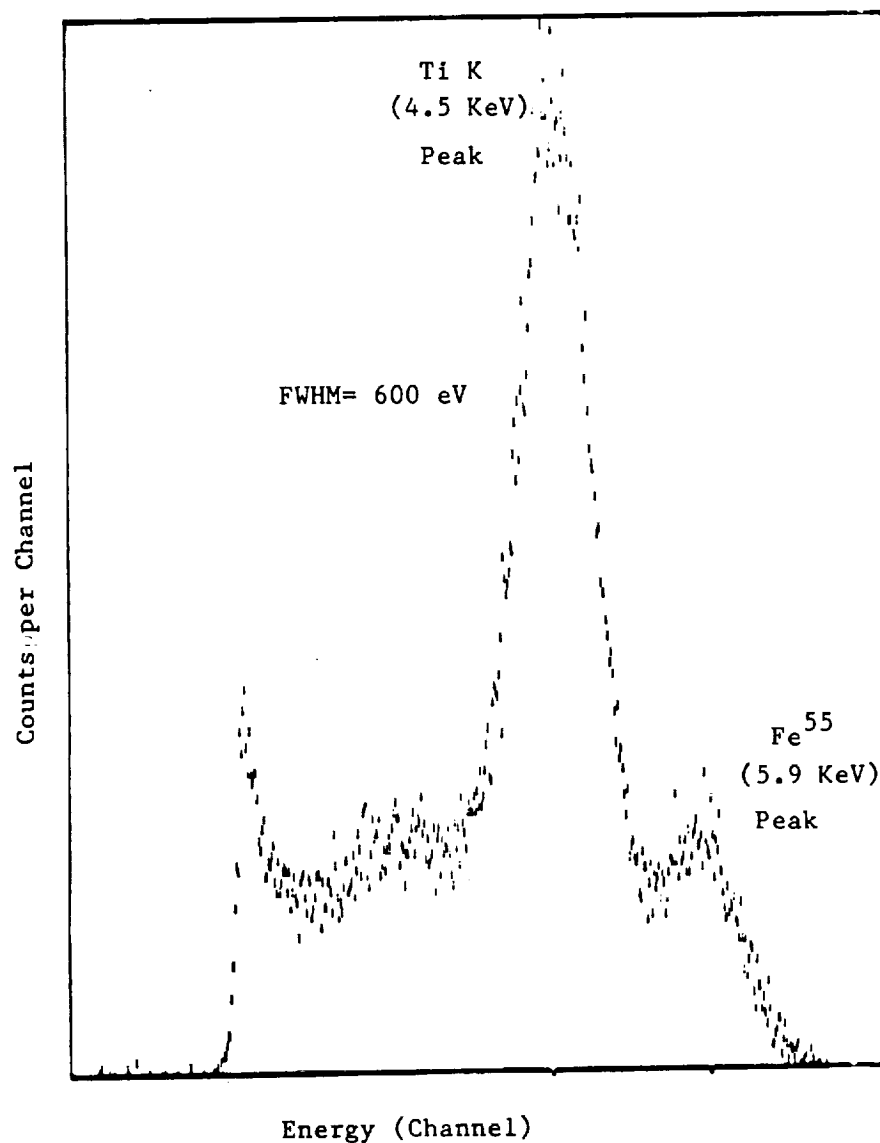


FIGURE 14

The Energy Spectrum Recorded Using a HgI₂ Detector, Upon Bombarding a Titanium Foil with X-rays from an Fe⁵⁵ Source

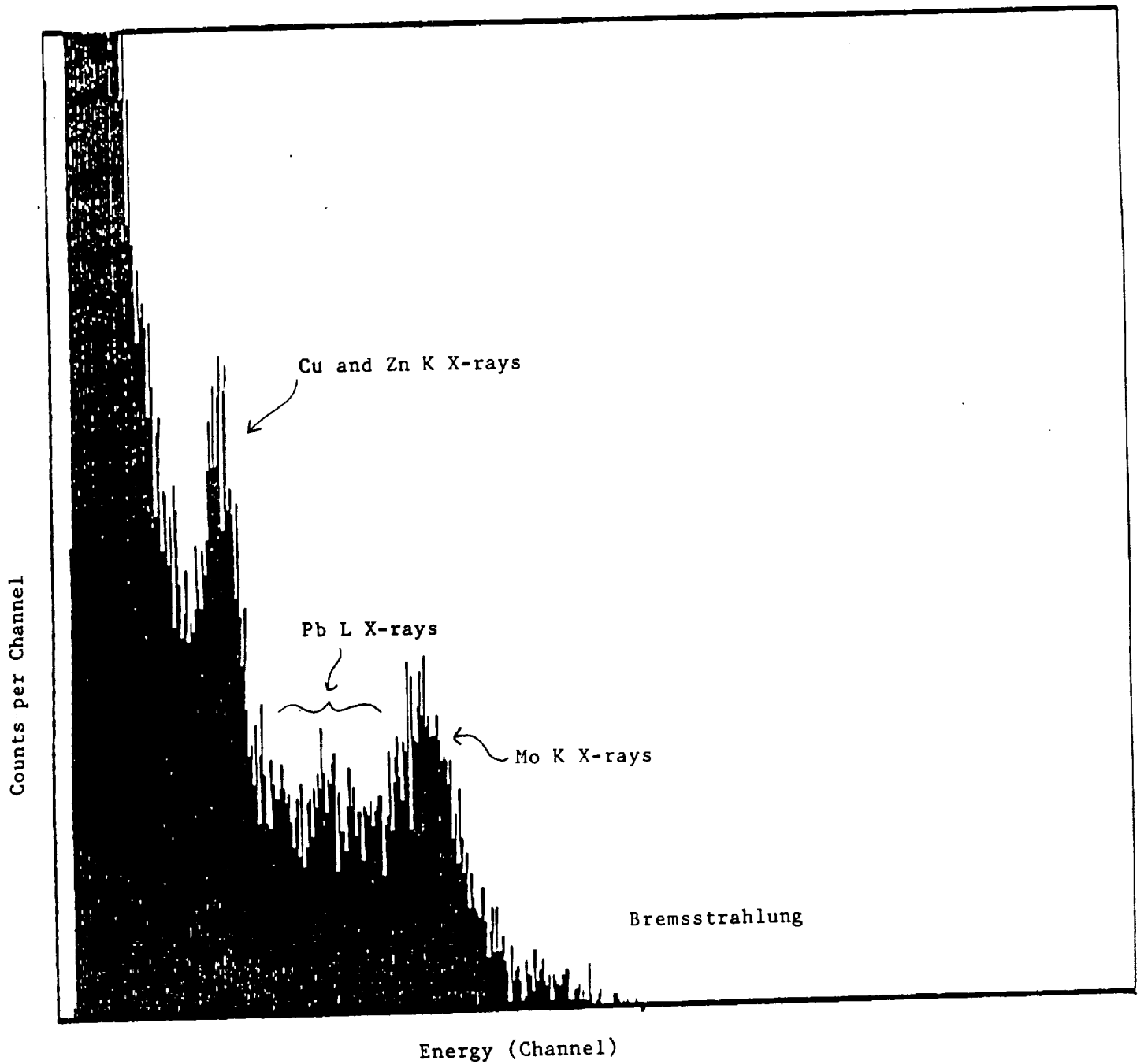


FIGURE 15
Output Energy Spectrum from an X-ray Machine Having a Mo Target, Recorded
Using a Mercuric Iodide Detector

the energy spectrum from a medical x-ray machine which had a molybdenum target. In view of very high flux from the machine, the detector was extensively collimated, with only a small fraction of active area exposed. The spectrum produced by the HgI₂ detector is reproduced in Figure 15. This experiment helped us in studying the changes in the spectrum produced by inserting different phantom films and demonstrated another practical application of the HgI₂ sensors.

IV. ENCAPSULATION EXPERIMENTS

A. Encapsulant Selection and Characterization - From the enormous number of possible candidates, a limited number of polymers were actively considered. The selection was made on the basis of several important criteria, which included low water and gas permeability in bulk, low x-ray attenuation as thin films, high electrical resistivity and chemical compatibility with mercuric iodide. Three important classes of encapsulants were explored: solution based polymers, vapor deposited polymers and plasma deposition polymers.

A variety of characterization techniques were used in order to investigate the utility of polymers as possible encapsulants. This included a specially designed copper diffusion test, electronic tests of coated devices under high temperature and vacuum conditions, scanning electron microscopy (SEM) of polymer films, and a permeability analysis of the encapsulants. A brief description of each technique is presented below.

1. Copper Diffusion Test - This test constituted a new characterization technique which was developed to detect HgI₂

penetration through various encapsulants. This test was found to be operationally easy and extremely sensitive and was based on the observation that HgI_2 reacts with a copper to form a dark compound. The rate of reaction was found to be relatively fast with first signs visible a few minutes after exposure to HgI_2 .

Several methods were investigated for determining porosity and/or high diffusion in the encapsulants. These included soaking in warm KI solution which dissolves HgI_2 through pin holes, placing the coated crystals in a 40°C temperature gradient under vacuum to force transport of any HgI_2 which penetrates through the encapsulant to the cold end, and testing by reaction with copper. The copper reaction was by far the most sensitive test and was performed as follows.

The experiment involved the use of a copper tape with the polished side laid adjacent to the encapsulated HgI_2 platelets. Another strip was laid on the other side to form a sandwich structure. The structure was then heated in an oven at 80°C . Failure of an encapsulant to prevent diffusion of HgI_2 was indicated by the appearance of a dark compound on the polished side of the copper tape. The intensity of the darkening indicated the effectiveness of the encapsulant. The test also revealed the presence of pin-holes in the encapsulants, which could be noticed from the lack of impressions left on the copper tape.

2. Permeability Analysis of Encapsulants - During the permeation of small molecules through a polymeric material, the rate of permeation depends on the parameters which are characteristic of the polymer and the transporting species. The ease with which a permeant passes through a barrier is referred to as "permeability". This general

term does not refer to the mechanism of the permeation but only to the transmission rate. On the basis of these considerations, it is possible to define permeability coefficient as follows: Permeability Coefficient \equiv (amount of permeant)/((area) x (time) x (driving force gradient)). The permeation of small gas molecules through polymer films occurs by consecutive steps of the solution of the permeant in the polymer and diffusion of the dissolved permeant. Consequently the permeability coefficient = diffusivity x solubility. Permeability is a complex function of various parameters involved in the polymer-permeant (gaseous) system, and has been shown to depend on many factors including polymer crystallinity, degree of cross-linkage in the polymer, size of gaseous species, thermal history of polymer, and temperature.

Permeability analysis of various encapsulants involved the characterization of encapsulants on the basis of their permeability values for gases and water vapor. Figure 16 shows a logarithmic scatter plot of permeability values of different encapsulants for oxygen and water-vapor permeation. Only polymers which exhibited sufficiently low gas and water vapor permeability were considered.

In addition, experiments were also conducted to characterize some plasma deposited films by evaluation of permeability of N_2 , O_2 and water-vapor on these films. Since plasma deposited films are extremely thin, about 1 micron, the experiment involved the use of a substrate polymer film of polyethylene, used as a support. Permeability was evaluated first for the substrate and then for the composite structure of substrate and deposited film. The permeability of the plasma film was back calculated. Figure 17 shows a schematic of the permeation cell

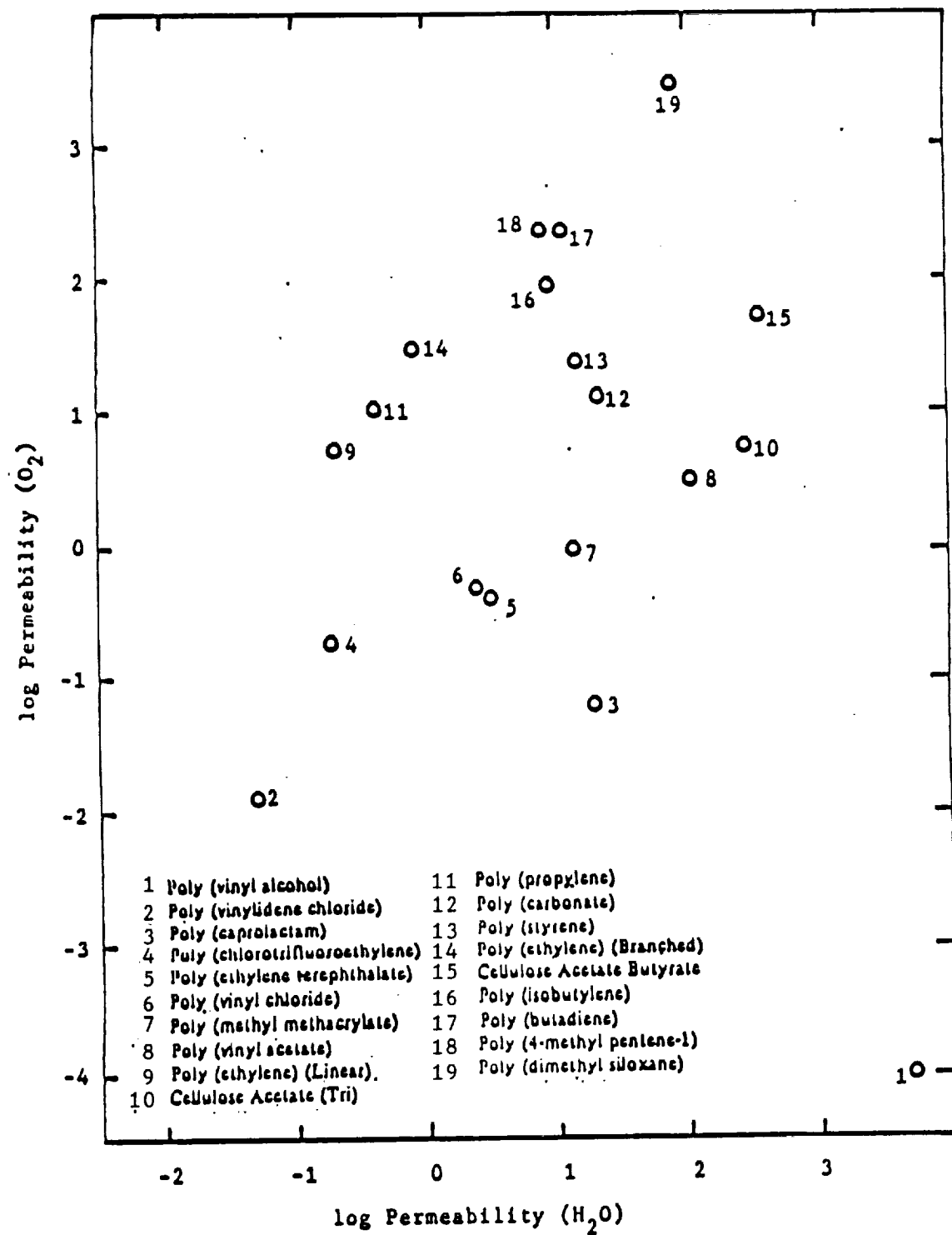


FIGURE 16
 Logarithmic scatter plot of the permeabilities to oxygen and water for a variety of polymers. Units are 10^{-11} cm²/sec-cm Hg.

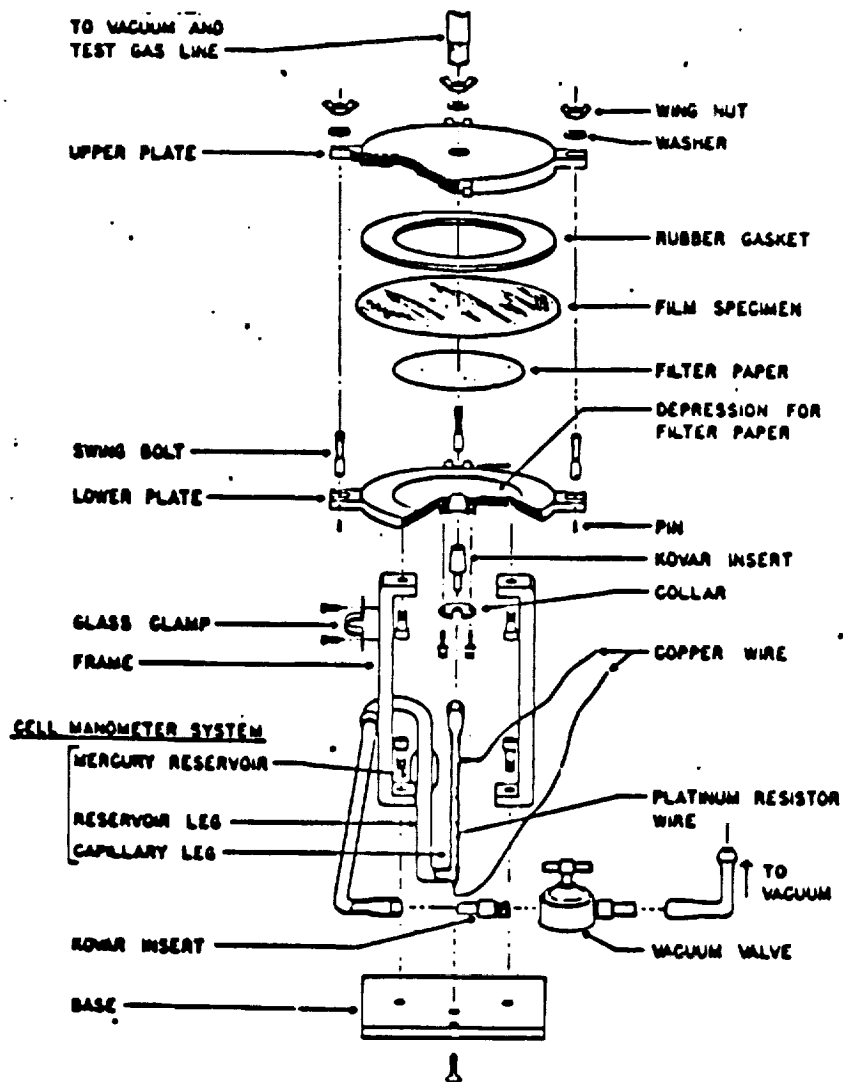


FIGURE 17

Schematic of a Permeation Cell Set-up

used. Table IV lists the measured permeability values for the plasma films and compares these values to literature values for other promising encapsulants.

3. Scanning Electron Microscopy - This technique was utilized to investigate and characterize plasma polymerized films. Experiments were performed at Eastern Analytical Laboratory in Massachusetts. The scans revealed the continuity and conformity of the films, nature of films around sharp edges and corners, film thickness and uniformity, and surface morphology. The films were also found to be pin-hole free which is an essential requirement. In addition to analysis of coated devices, behavior of plasma deposited films around sharp edge of a razor blade was also studied.

B. Accelerated Testing Under High Temperature and Vacuum

1. Theoretical Diffusion Model - Diffusion was believed to be a principal component in the degrading mechanism of HgI_2 devices. The extent of diffusion would determine the rate of the degradation process. A theoretical model was developed to predict the mass transfer rate of HgI_2 through the encapsulant and thereby gain an insight into the degradation process.

The assumptions made in developing the model were:

1. Steady state conditions exist
2. Unidirectional mass transfer
3. Constant physical parameters (e.g., diffusivity and permeability)

A mass balance for HgI_2 was taken over a control volume and the resulting differential equation was integrated over the entire

TABLE IV
Permeability of Polymer Films to Water Vapor (25°C)

Film	Permeability (P) $\frac{\text{cm}^3(\text{STP}) \cdot \text{mm} \times 10^8}{(\text{cm}^2 \cdot \text{s})(\text{cm Hg})}$
Polyethylene	13
HB6 acrylic	10
Plasma - Standard	7
Parylene C	5
PVDC	0.3-1.0
Plasma - Modified	0.3

volume to give the following expression predicting the mass transfer rate

$$Q = AXMP \quad (3)$$

where Q is the mass transfer rate

M is the permeability of HgI_2 in the polymer

P is the vapor pressure of HgI_2

A is a geometrical factor

This quantitative analysis provided further insight in designing accelerated testing conditions. As the operating temperature is raised, both the vapor pressure (P) of HgI_2 and the permeability (M) of polymer increase. On the basis of this, a dimensionless factor of acceleration (g) was defined:

$$\begin{aligned} g &= Q_1/Q_2 = M_1P_1/M_2P_2 \\ &= \exp (E/RT_1 - E/RT_2)P_1/P_2 \end{aligned} \quad (4)$$

where subscript 1 refers to values of parameters at temperature T_1 and subscript 2 to values of parameters at temperature T_2 . E refers to the activation energy of diffusion and R to the ideal gas constant. Value of E was approximated to be 2.65 Kcal/mole (value for CO_2 diffusion in silicone rubber) (13). Selecting $T_1 = 373$ K and $T_2 = 295^\circ K$ and substituting values in Equation 4 gives a factor of acceleration, $g = 50$ at $80^\circ C$ and $g = 200$ at $100^\circ C$.

This calculation indicates that if a device worked for a day at $100^\circ C$, it can work for 200 days at $22^\circ C$. Thus the rate of degradation is about 200 times faster at $100^\circ C$ as compared to $22^\circ C$.

2. Accelerated Testing - Experiments were performed subjecting the coated devices to high temperature conditions ($80^\circ C$) and comparing

the device performance before and after heating. During more rigorous testing, high temperature conditions were coupled to vacuum environment and the device performance was subsequently recorded. Accurate recording of leakage current, energy resolution and peak-to-valley ratio on the low energy side provided a basis to observe minute variations in device performance, which would signify device degradation. Devices were also observed under a microscope to check for apparent variation and occasionally showed a collection of tiny HgI_2 granules on the polymer film, indicative of high temperature thermal degradation.

3. Comparison of Accelerated Testing to Long Term Testing - No encapsulation scheme is of value unless it can be shown with reasonable certainty that it will survive long periods of time. It is obviously unsatisfactory to wait long periods of time to confirm this. Therefore it was necessary to develop a reliable accelerated test procedure which could be shown to correlate well with the effects which occur with the actual passage of time. Because of our earlier research on HgI_2 devices prior to Phase I of this effort, we had a small variety of encapsulated crystals which could serve to validate accelerated techniques designed here. A direct comparison of long term aging and accelerated aging was possible for several types of encapsulant.

To perform the test, coated crystals were through a series of temperature cycles, heated under vacuum, and exposed to light. We determined that in spite of the destructive phase transition which occurs in HgI_2 at 125°C and its high vapor pressure, encapsulated crystals could be heated without damage if the maximum temperature used was less than 100°C . As discussed below, we observed that these

processes did accelerate changes in the coated crystals and that these changes correlate well to effects observed on crystals which were encapsulated 2 years earlier.

Figures 18 b,d,e and f show the results of accelerated testing on a number of crystals coated with various materials. Three different effects were observed: reaction, dissolution, or no change. The observations made on crystals which had been coated two years earlier gave us invaluable information to test the validity of our accelerated methods.

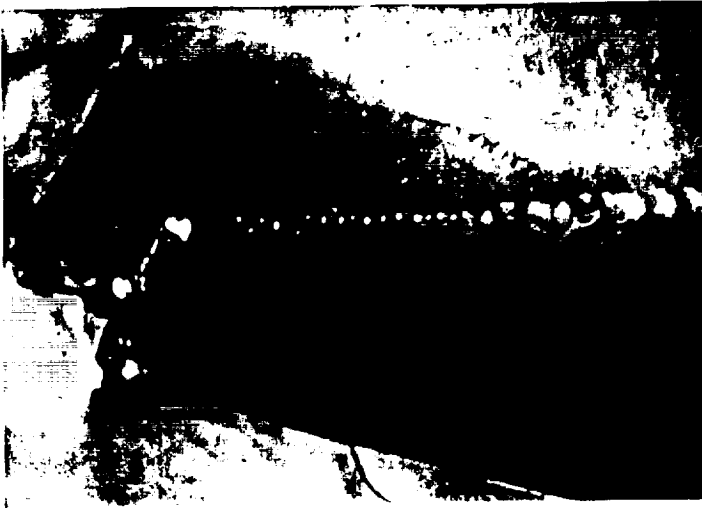
Figure 18 a and b compare a crystal which reacted to form a brownish-green material on its surface under the accelerated conditions to a similar result obtained for the same encapsulant after two years storage under ambient conditions. In this case the accelerated test was complete in four days. The encapsulant used was a urethane.

Figures 18 c and d show crystals which dissolved in the encapsulant to the extent that holes formed. Long term testing and seven days of accelerated aging again gave similar results. The encapsulant used was an acrylic.

Figures 18 e and f show encapsulated crystals which survived the seven day accelerated aging process unchanged. The encapsulant used in Figure 3 was HB-6, an acrylic. The encapsulant used in Figure 18f was custom formulated in-house using polyethylene. These results are extremely important, since the validity of the accelerated test was confirmed.

C. Encapsulant Studies

1. Solvent Based Encapsulants - In our early search for



a) HgI_2 crystal coated with IIA-2 after 2 years. Note brownish precipitate.



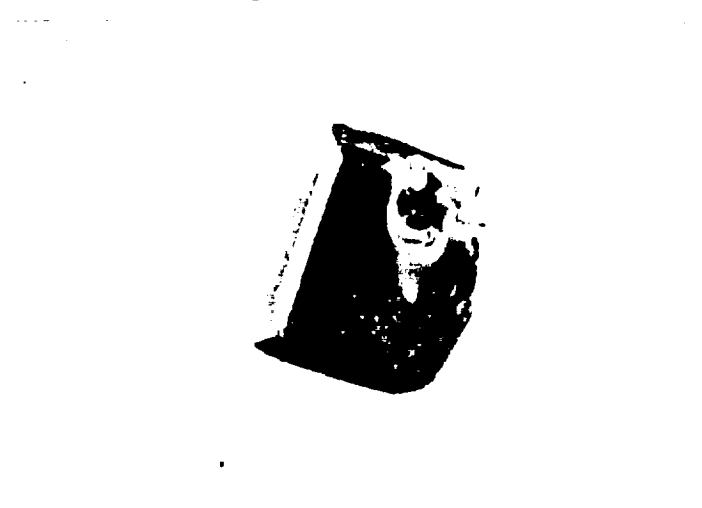
b) HgI_2 crystal coated with HA-2 after accelerated testing.



c) HgI_2 crystal coated with HB-1 after 2 years. Note holes where it dissolved in the coating.



d) HgI_2 crystal coated with HB-1 after accelerated testing.



e) HgI_2 crystal coated with IIB-6 after accelerated testing. No change.



f) HgI_2 crystal coated with polyethylene after accelerated testing. No change.

FIGURE 18

possible encapsulants, we had decided to examine polymers that could be applied to HgI_2 devices by simple methods such as dip coating and spraying. Polymers were chosen on the basis of their solubility in common solvents, their gas and water permeability and their chemical compatibility with HgI_2 . Upon testing, most of the solvent based polymers that we applied by these simple methods were shown by our copper diffusion test to be unsuitable for long term use.

There appears to be a significant inherent problem in using solvent-based encapsulants. The solvents which were needed for the best polymers also dissolved HgI_2 . One polymer that showed great promise was polyvinylidene chloride which has excellent diffusion barrier properties. However dissolving it into a usable liquid form required polar solvents such as MEK which also dissolved HgI_2 . Another promising candidate was Neocryl -723 acrylic dissolved in toluene, which dissolved HgI_2 slowly. Acrylic polymers generally have moderate permeability and the Neocryl passed the copper diffusion test. However, working devices coated with the material usually failed, suggesting a failure mechanism consistent with dissolution of HgI_2 . Table V summarizes the results and shows that most of the possible candidates were eliminated because they failed the sensitive copper diffusion test.

The best polymer identified in this class of encapsulants was Humiseal HB6 which, when deposited in thick layers, passed all of our accelerated testing. One of the devices coated with this encapsulant functioned without any degradation for 9 months. However, when we attempted to prepare thin films we not only encountered the solvent problems, but had difficulty in obtaining thin uniform films which could

TABLE V
Summary of Encapsulant Data--Liquid Based Polymers

Polymer(solvent)	Method of Application	Reactions -In presence of copper tape(Heated unless otherwise indicated) -Other reactions	Actual Devices Coated
HB6 acrylic (toluene)	-dropped on -spray	black Cu compound	-one device lasted over 10 months -other sprayed devices degraded
Saran F-310 PVDC (MEK)	spray	-black compd -heat caused Saran to turn brown	none
Saran F-310 (1:1 toluene/MEK)	dropped on	black compd	none
Saran F-310 (n-butyl acetate)	dropped on	black compd	none
Saran F-310 (cyclohexanone)	spray	black compd	working devices degraded slightly
DATAKOAT gloss acrylic spray		no reaction(unheated)	none
Scotch-gard	spray	black compd	none
lacquer	spray	-black compd -left a shell in polymer behind	none
polyurethane varnish	spray	-left a shell in polymer behind -polyurethane turned yellow upon heating	none
HB15 acrylic	spray	black compd	none

Summary of Encapsulant Data--Liquid Based Polymers (continued)

HA27 polyurethane	spray	black compd	none
Enamel E-1757	dropped on	black compd	none
Neocryl A-622 acrylic(water)	dropped on	small amount of black compd(unheated)	none
Neocryl B-723 acrylic(toluene)	dropped on	no reaction	working devices failed after application
Neocryl B-723LV acrylic(toluene)	dropped on	no reaction	none
Neocryl B-745 acrylic(toluene)	dropped on	black compd	none
Synthemul 90-608 acrylic(water)	dropped on	black compd	none
Synthemul 97-467 acrylic(water)	dropped on	black compd	none
Synthemul 97-731 acrylic(water)	dropped on	no reaction on copper tape but crystal is surrounded by yellowish compd	none
Krylon Electronic Acrylic Crystal Clear Spray		black compd	none

pass the copper diffusion test. About half of the devices coated with thin films failed this test.

Because of the solvent problems and the lack of control of the simple deposition methods, we decided to pursue nonsolvent deposition methods such as the parylene-C process and the plasma polymerization process.

2. Parylene Coatings - Parylene is a generic name of a series of thermoplastic polymers developed by Union Carbide Corporation. The basic constituent of this series is poly-para-xylylene. The member of this series that was selected for the present application was Parylene C (poly mono chloro para xylylene) because of its superior resistance to mass transfer and low x-ray attenuation. We had our devices custom coated with Parylene C by Novatran Corp., N.H. This coating operation involved the vapor phase transport of constituent monomer and the subsequent polymerization on the crystal surface. The operation produced a uniform, conformal coat of the polymer with the film thickness of 5 microns.

Usually materials to be coated with Parylene are pre-treated with an organic silane as a part of the licensed process. The sample undergoes a silane deposition step during which a layer of organic silane is formed on the sample surface by a vapor transport process. This silane layer subsequently acts as a polymerization site for the incoming monomer of Parylene.

Due to the possibility of mechanical damage to the HgI_2 crystals imparted by the silane layer and the contaminating nature of organic silanes, we bypassed the silane treatment in half of our

samples. Optical examination of the samples treated with silane showed collection of dust-like particles in polymer films and a large number of dark spots on the crystal surface. In contrast the detectors which did not undergo the silane treatment appeared clear and clean. Since the adhesive between the Parylene film and the crystal surface appeared to be satisfactory, the silane pre-deposition step can be safely avoided.

The results of the test run involving Parylene deposition were very encouraging. The spectrum produced by a detector, showing ^{55}Fe peak, remained unchanged after the encapsulation process. Parylene coated device also passed the copper diffusion test and coated device has been functioning for a year without degradation. accelerated testing of a Parylene coated detector at 80°C for a week has been successful. Thus Parylene seems to be a very promising encapsulant. There is some evidence that the encapsulant may be causing mechanical damage to the fragile crystals.

3. Plasma Polymerized Encapsulants - Plasma polymerization was investigated as a means of depositing inert polymers on HgI_2 devices. The important advantages offered by plasma polymerized films are elimination of solvent effects, pin-hole free surfaces, ease of control of film thickness and uniformity of films. In addition, the plasma polymerized films possess a highly cross linked structure and hence excellent chemical diffusion resistance.

The technique utilized for generating plasma induced polymerization was glow discharge, where free electrons gain energy from an imposed electric field and lose it subsequently through collisions with monomer gas. These collisions lead to formation of a host of

reactive species, some of which become precursors in the resultant polymerization reaction. This condition leads to the deposition of thin films directly onto the surface of the substrate. In this process, the deposition occurs at near room temperature and no damage occurred to the HgI₂ devices during the coating operation. Coating operation was carried out at Plasma Physics Corp., N.Y. Figure 19 shows a schematic of a plasma deposition system. *

We examined two encapsulant recipes for the plasma polymerization process. These were the "standard" plasma films which had a hydrocarbon structure and modified plasma films which were optimized to give thicker (2 microns) films on HgI₂ devices.

The standard plasma films showed a surprisingly high volume resistance (greater than 10¹⁸ ohm-cm). It also exhibited excellent adhesion to varied surfaces. Devices coated with about 1-2 microns of this encapsulant have been functioning now for 14 months at the time of this report without degradation. This encapsulant has passed our copper diffusion test. Also, 67% of the devices coated with this encapsulant have showed no degradation in performance when heated to 80°C for 1 week. Table VI compares the performance of this encapsulant at room temperature with other promising polymers. Table VII presents the results for high temperature and vacuum conditions. Using SEM the films of this polymer were revealed to be continuous, uniform and devoid of pin-holes when investigated using SEM, as shown in Figure 20. Thus this encapsulant shows great promise as a barrier material.

The modified plasma films also possessed very high electrical resistivity (greater than 10¹⁸ ohm-cm). In addition, it was found to be *

- A - Variac
- B - Transformer
- C - Electrodes
- D - Manifold
- E - Flowmeters
- F - 3 way stopcock
- G - Gauge
- H - Plasma Chamber
- I - Cold trap
- J - Pump

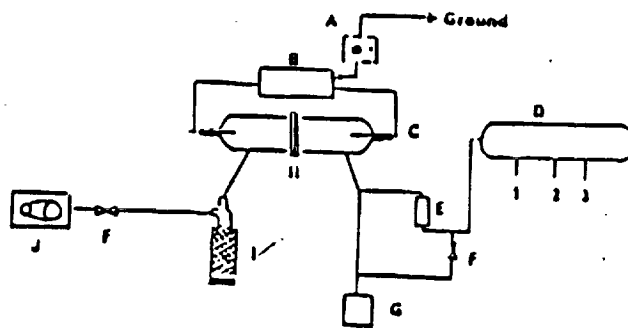


FIGURE 19

A typical plasma system.

TABLE VI
Room Temperature Stability Analysis

Number of Encapsulated Devices Remaining Stable As a Function of Time

Encapsulant	Onset	1 Month	3 Months	6 Months	9 Months	12 Months
None	25	12	3	0	0	0
Urethanes	8	3	2	0	0	0
Silicones	21	14	9	2	0	0
Acrylics	15	11	8	6	6	5
Parylene C	2	1	1	1	1	1
Plasma-Standard	14	14	14	14	13	13
Plasma-Modified	15	15	15	15	15	15

TABLE VII
High Temperature Stability Analysis

Encapsulant	Test Conditions			No. of Devices	% Pass (no Degradation)
	Temperature	Duration	Vacuum		
Acrylics	80°C	7 days	atm.	4	0
Parylene C	80°C	7 days	atm.	1	100%
Plasma-Standard	80°C	7 days	atm.	6	67%
Plasma-Modified	80°C	7 days	atm.	6	100%
Plasma-Standard	80°C	7 days	150 μ Hg	6	50%
Plasma-Modified	80°C	7 days	150 μ Hg	5	100%
Plasma-Modified	80°C	14 days	100 μ Hg	10	100%
Plasma-Modified	100°C	45 days	100 μ Hg	4	75%



FIGURE 20

Scanning Electron Micrograph of a Coated
Detector

extremely inert to chemicals and solvents. It demonstrated very high thermal and vacuum stability. These unique properties of the polymer can be attributed to its structure.

This encapsulant passed our copper diffusion test. In addition devices coated with it have been functioning for 13 months without any degradation (at the time of this report). All the devices were subjected to high temperature (80°C) and vacuum (100 microns of H_g) for 2 weeks, after which all performed without any change. *

Permeability of this encapsulant was found to be lowest among all encapsulants considered and SEM investigation of these films revealed continuous, conformal and pin-hole free structures.

During a plasma run, we had coated a razor blade with this encapsulant to study the nature of these films around edges and corners. Figure 21 shows a SEM of this razor blade, showing that the film completely covers the fine edge of the blade. Thus the SEM conclusively demonstrated that these films maintain continuity and conformity around sharp edges which is crucial from the viewpoint of the current application when considering the edge of the device, the contact and the contact leads.

All these properties and performance characteristics indicate that this encapsulant has essentially solved the HgI₂ stability problem.

V. CONCLUSIONS

For many years HgI₂ has appeared to be an ideal material for use in uncooled x-ray and gamma ray detectors. This is because it is a wide band gap semiconductor which permits room temperature operation. It has

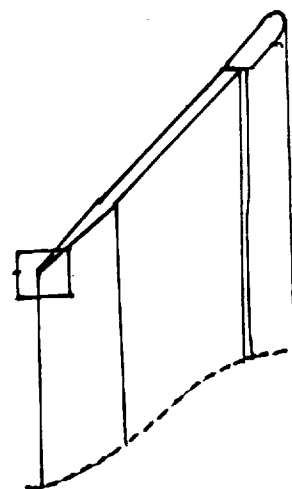
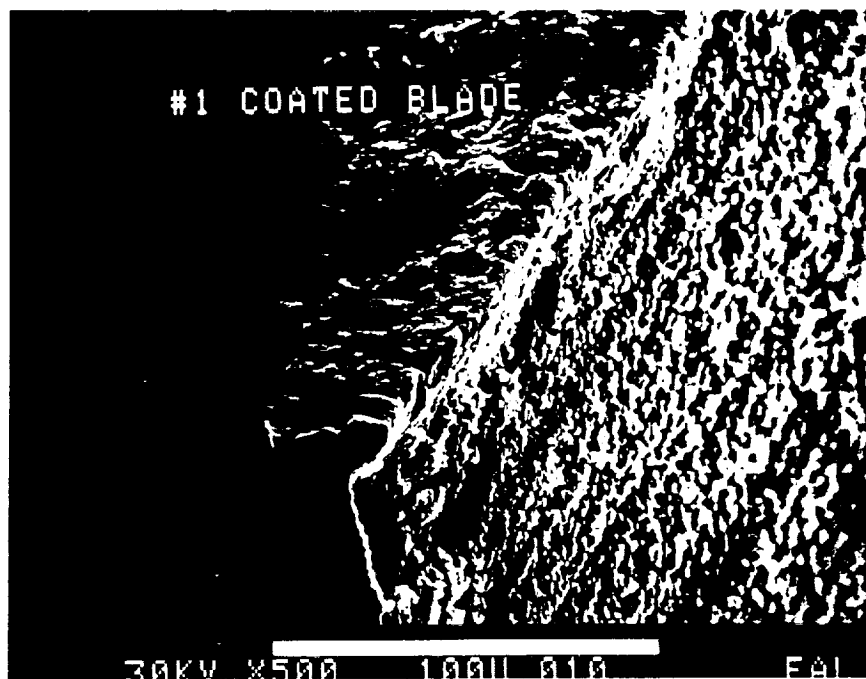


FIGURE 21

SCANNING ELECTRON MICROGRAPH OF A PLASMA COATED RAZOR BLADE

a high average atomic number and high density which gives it very good stopping power for x-rays and gamma rays. Most importantly, crystals can be grown with excellent electronic properties including moderately good electron and hole transport and high sensitivity. These are exactly the properties needed for making sensitive, low noise, solid state x-ray sensors.

HgI₂ devices, however, have been plagued by instability problems which have prevented their use. Detector performance degrades rapidly after fabrication, often within a few days or weeks. HgI₂ technology has matured to the point where excellent crystals and devices can be produced by a number of techniques. In addition, recent advances in low noise electronic preamplifiers has made the construction of sensitive, high resolution HgI₂ spectrometers possible. Thus, device instability was the major remaining obstacle which prevented the implementation of useful HgI₂ based instrumentation.

Standard packaging and encapsulation techniques have failed to protect HgI₂ devices for a variety of reasons but the details of the failure mechanisms were not clear. Solving this problem required gaining a better understanding of the mechanisms responsible for device failure and demonstrating that the proper selection of encapsulation technique could significantly improve the operating life of HgI₂. To achieve this, we developed accelerated testing methods and tested a variety of encapsulant types to determine their stability and suitability for use with HgI₂. The chemical, physical, and mechanical properties of the encapsulants were also examined.

The results of this effort include a better understanding of the

mechanisms responsible for HgI₂ device failure and their dependence on encapsulant type and a significant increase in crystal stability. This should translate to a potential device life of up to twenty years or more. The significance of these results are far reaching. Stable HgI₂ sensors will not only permit this technology to finally be used in satellite systems but will also provide sensors for many applications. These include room temperature laboratory instruments, portable x-ray fluorescence spectrometers and industrial nuclear gauging equipment.

VI. REFERENCES

1. G. F. Knoll, "Radiation Detection and Measurements", John Wiley and Sons (1979).
2. G. A. Armantrout, et. al, "What Can be Expected From High-Z Semiconductor Detectors", IEEE Trans. Nucl. Sci., 29, 121 (1979).
3. J. S. Iwaczyk, A. J. Dabrowski, G. C. Huth, and T.E. Economou, "measurement of the Characteristic X-ray of Oxygen and Other Ultrasoft x-rays using Mercuric Iodide Detectors", Appl. Phys. Lett., 46 (6), 606 (1985).
4. J. S. Iwaczyk, J.G. Bradley, J.M. Conley, and A. L. Albee, "Low Energy X-Ray Spectra Measured With a Mercuric Iodide Energy Dispersive Spectrometer in a Scanning Electron Microscope", IEEE Trans. Nucl. Sci., 33 (1) (1986).
5. J.S. Iwaczyk, A.J. Dabrowski, and G.C. Huth, "Continuing Development of Mercuric Iodide X-Ray Spectrometry", Adv. X-Ray Analysis, 27, 405 (1984).
6. NASA Contract Number NASW-3437, "Mercuric Iodide X-Ray Detectors

for NASA Flight Applications:.

7. M. Schieber, I. Beinglass, G. Dishon, and A. Holzer, "Growth of Large Crystals of HgI_2 from the Vapor Phase by the Temperature Oscillation Method", Crystal Growth and Materials, edited by E. Kaldis and H.J. Schel, North Holland Publ. Company (1977).

8. C.C. Coleman, J. Crystal Growth, 203 (1970).

9. N. Rama Rao, J.K.D. Verma, and A.P. Patro, J. Physics, 13, 1545 (1980).

10. H. Scholz, Acta Electronica, 17, 69 (1974).

11. M. R. Squillante, S. Lis, T. Hazlett; and G. Entine, "State of the Art X-ray Detectors Fabricated on PCG Grown Mercuric Iodide Platelets:", Mat. Res. Soc., 16, 191 (1983).

12. K. Hecht, Z. Physik, 77, 235 (1932).

13. J. Comyn, "Polymer Permeability:", Elsevier Appl. Sci. Publishers (1985).